

# Discrete curvature on graphs from the effective resistance

Karel Devriendt\*

University of Oxford, UK

Alan Turing Institute, UK

Renaud Lambiotte†

University of Oxford, UK

Alan Turing Institute, UK

January 2022

## Abstract

This article introduces a new approach to discrete curvature based on the concept of effective resistances. We propose a curvature on the nodes and links of a graph and present the evidence for their interpretation as a curvature. Notably, we find a relation to a number of well-established discrete curvatures (Ollivier, Forman, combinatorial curvature) and show evidence for convergence to continuous curvature in the case of Euclidean random graphs. Being both efficient to calculate and highly amenable to theoretical analysis, these resistance curvatures have the potential to shed new light on the theory of discrete curvature and its many applications in mathematics, network science, data science and physics.

## 1 Introduction

The idea of curvature has a long and rich history in geometry and provides the mathematical language for one of the most important physical theories, Einstein’s theory of general relativity, which describes the interplay between mass and energy and the (Ricci) curvature of spacetime. As illustrated in Figure 1, curvature is a geometric property of smooth spaces such as lines and surfaces, which aims at characterising how a space differs from flat Euclidean space and can be understood intuitively via the dispersion of its geodesics, with geodesics remaining parallel in a flat space with zero curvature, converging in a spherical space with positive curvature or diverging in a hyperbolic space with negative curvature. Recently, the question to formulate an analogous theory of *discrete curvature* for non-smooth objects and structures such as graphs or meshes has gained a lot of attention. Some important reasons for this growing interest can be found in the ubiquity of discrete data following the advent of digital technologies, manifest both in industry and science, in the ongoing efforts to develop a theory of quantum gravity, where questions on discrete curvature naturally arise when combining the continuous theory of gravity and the discrete theory of quantum mechanics, and finally in the successful development of a number of broadly applicable notions of discrete curvature. Broadly speaking, the vision is that discrete curvature can play an important role in representing and understanding ‘emergent’ geometric properties in discrete structures – which at the local level appear purely combinatorial but at a larger scale feature much richer properties. Within network science for instance, important applications include community detection [54, 61], methods to hinder bottlenecks in graph neural networks [67] and alternative ways to capture connectivity in interconnected systems [74, 52, 36, 53]

In this article, we propose a new approach to discrete curvature on graphs which differs fundamentally from existing approaches and is based on effective resistances, a concept intrinsically

---

\*Contact: karel.devriendt@maths.ox.ac.uk – Funding: KD was supported by The Alan Turing Institute under the EPSRC grant EP/N510129/1.

†Funding: RL acknowledges support from the EPSRC Grants No. EP/V013068/1 and No. EP/V03474X/1.

linked to electrical circuits and other linear systems [3] and with many graph-theoretic properties. The introduced *resistance curvatures*, one for nodes (vertices) and one for links (edges), are very simple to state and efficient to calculate, but at the same time come with a wealth of theoretical properties which make them a promising contribution to the theory of discrete curvature and of network geometry [9] more generally. To evidence our measure as a valid notion of curvature, we show its relation to existing notions of discrete curvature (Ollivier-Ricci, Forman-Ricci and combinatorial curvature) and we show evidence that it converges to its continuous curvature counterpart in the case of Euclidean random graphs. As an example application, we show how this curvature has a naturally associated discrete Ricci flow which is formally related to existing models of social balance in social dynamics.

The rest of the article is structured as follows: Section 2 introduces the concept of curvature and the necessary definition on graphs and the effective resistance. In Section 3, the new resistance curvature is introduced with some basic properties and a number of examples. Section 4 discusses the different arguments that support our introduced definitions as discrete curvatures and Section 5 treats the associated discrete Ricci flow. In Section 6, finally, we conclude the article with a brief summary and discussion. Proofs and further technical results are presented in the Appendix.

## 2 Preliminaries

### 2.1 Continuous and discrete curvature

The classical setting of curvature is differential geometry [37, 7], where it characterizes how much and in which ways a smooth space differs from being flat around a point. *Scalar curvature* for instance associates a single number to each point on a manifold and allows to distinguish the qualitatively different cases of positive curvature (like the surface of a sphere), zero curvature (like the flat plane) and negative curvature (like a saddle point), as illustrated in Figure 1. The scalar curvature is a measure of how much the volume of (small)  $\epsilon$ -balls around a point differ from the volume of  $\epsilon$ -balls in Euclidean space of the same dimension. *Ricci curvature*, on the other hand, associates a tensor to each point on a manifold, and reflects the difference of volume growth between geodesics emanating from the point in two tangential directions compared to Euclidean growth. While the Ricci curvature includes ‘directional’ information not present in the scalar curvature, the latter can be retrieved as the trace of the former. We refer the readers to [37, 7] for references on curvature and differential geometry.

While discrete spaces such as graphs lack the differential structure required for classical definitions of curvature, it is still widely acknowledged that these spaces exhibit relevant geometric features and consequently, there have been many attempts at formulating a theory of *discrete curvature* that works in these generalized settings as well [16, 26, 5, 55, 60]. The idea of discrete curvature is perhaps most easily understood in the case where the discrete spaces under consideration are closely related to some smooth space, for instance a graph which can be isometrically embedded into a manifold (see Section 4.1) or random geometric graphs which are natural ‘coarse’ representations of some smooth space (see Section 4.3). However, even when there is no clear underlying or latent smooth space involved, discrete notions of curvature can be formulated. Importantly, most contributions on the subject of discrete curvature not only attempt to generalize the definition of curvature, but also try to translate the multitude of curvature-related results over to this new setting. For more information on different approaches to discrete curvature and their theory, we refer the reader to [39, 58]. In Section 4.2 we give a short introduction to combinatorial curvature, Ollivier-Ricci curvature and Forman-Ricci curvature, as these particular notions are related to our proposed curvature.

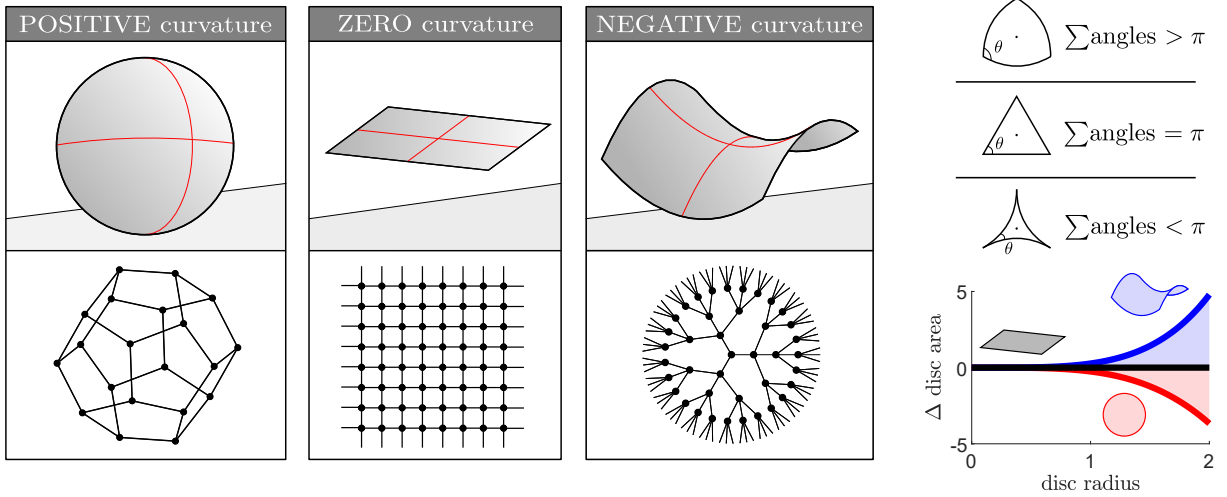


Figure 1: *Scalar curvature distinguishes points with different local geometries. On smooth surfaces, such as the images shown on the left, points with positive/zero/negative curvature are locally like the surface of a sphere/flat plane/saddle point. On the right is illustrated how the curvature sign influences the local geometry around a point, in terms of triangles around the point (with different angle sums) and in terms of volume growth (where geodesic discs can grow faster/slower than in Euclidean space). The second row on the left shows some graphs which are naturally associated to spaces of constant curvature, see Section 4.1.*

## 2.2 Graphs, Laplacians and the effective resistance

Here, we introduce the preliminaries on graphs and effective resistances required to define the resistance curvature; further details can be found in [18]. While we mainly work in the setting of *weighted graphs*, it is important to note that a weighted graph is nothing more than a set together with some notion of similarity defined between (some) pairs of elements of this set. This type of data is of course very general and widely available, which broadens the applicability of the resistance curvature to more than just graph theory and network science. For instance, any dataset with a similarity kernel – or a parametrized family of kernels to cover different scales, as is often the setting in TDA [28, 13] – will naturally have an associated weighted graph whose resistance curvature then says something about the geometry of the underlying dataset. This is illustrated by the analysis in Section 4.3, where we find that the resistance curvature (calculated via an associated graph) retrieves the flat curvature of a point-set in the Euclidean plane.

A weighted graph  $G = (\mathcal{N}, \mathcal{L}, c)$  consists of a set of  $n$  nodes  $\mathcal{N}$  and a set of  $m$  links  $\mathcal{L}$  that connect pairs of nodes<sup>1</sup>, denoted by  $(i, j) \in \mathcal{L}$  or simply  $i \sim j$ . Furthermore, each of the links is assigned a positive weight through the function  $c : \mathcal{L} \rightarrow \mathbb{R}_{>0}$  and we write  $c_{ij}$  for the weight of a link  $(i, j)$ . We furthermore restrict our attention to *simple, undirected graphs without self loops*. One convenient way to describe and study weighted graphs is by their associated Laplacian matrix. For a given  $n$ -node graph, the *Laplacian matrix* is an  $n \times n$  matrix  $Q$  whose rows and columns are identified with the node set  $\mathcal{N}$ , and with entries

$$(Q)_{ij} := \begin{cases} -c_{ij} & \text{if } i \sim j \\ k_i & \text{if } i = j \\ 0 & \text{otherwise,} \end{cases}$$

<sup>1</sup>Traditionally, nodes and links are often referred to as vertices and edges instead. We choose to work with “nodes and links” to describe graphs and reserve the terminology of “vertices and edges” to describe simplices which appear in the study of effective resistances, see for instance [24, 18]. To avoid confusion, we also note that our notion of link is distinct from the “link of a simplex” in the context of simplicial complexes

where  $k_i := \sum_{j \sim i} c_{ij}$  is the *weighted degree* of node  $i$ , i.e. the total weight of all links incident on node  $i$ . We will also be interested in the *combinatorial degree* of a node  $i$ , which is defined as  $d_i := \sum_{j \sim i} 1$  and is independent of the link weights. Apart from being a convenient matrix representation of the data associated to a weighted graph, the Laplacian matrix is also a central object in (spectral) graph theory [15, 49, 48] with broad applications [34, 69, 62, 17, 70].

The Laplacian matrix is positive semidefinite and its rank depends on the number of connected components  $\beta(G)$  in the graph as [15]

$$\text{null}(Q) = \beta(G) \text{ or } \text{rank}(Q) = n - \beta(G),$$

where the kernel is spanned by vectors which are piecewise constant on the components of  $G$ ; we write  $G_i$  to denote the unique connected component that contains a given node  $i$ . In context of this article, the Laplacian is mainly relevant for its relation to the effective resistance. This resistance is defined based on the *Moore-Penrose pseudoinverse* of the Laplacian  $Q^\dagger$ , which is determined by the equations  $Q^\dagger Q = Q Q^\dagger = \text{proj}(\ker(Q)^\perp)$  and can be calculated, for instance, by inverting the nonzero eigenvalues of the Laplacian matrix.

The *effective resistance* between pairs of nodes is defined based on this pseudoinverse Laplacian as

$$\omega_{ij} := (\mathbf{e}_i - \mathbf{e}_j)^T Q^\dagger (\mathbf{e}_i - \mathbf{e}_j), \quad (1)$$

for any  $i, j$  in the same connected component<sup>2</sup>, where  $\mathbf{e}_i$  is the  $i^{\text{th}}$  unit vector. The concept of effective resistances originates from the theory of electrical circuits, where it captures the resistance exerted by the whole network on a current flowing between any two nodes [20]. The effective resistance has many mathematical properties and one of its most celebrated properties is that it is a metric between the nodes of a graph, see also [18]:

**Theorem 1** (Resistance is distance [33, 42]). *The effective resistance is a metric between the nodes of a graph.*

Theorem 1 provides a good way to think intuitively about effective resistances: if  $\omega_{ij}$  is large, this reflects that nodes  $i$  and  $j$  are not well connected in the network – there are few and mainly long paths connecting  $i, j$  –, whereas a small  $\omega_{ij}$  means that they are well connected – there are many short paths between  $i, j$ . The effective resistance thus reflects a more integrated notion of distance compared to the shortest path distance, since it takes into account all the different paths between two nodes and how they are interconnected.

In this article, we will mainly be interested in the product of the link weight and the effective resistance between the end nodes of the link,  $c_{ij}\omega_{ij}$  which we call the *relative resistance*<sup>3</sup> of  $(i, j)$ . This relative resistance reflects the *importance* of a link for connectivity of the graph. A link which is very redundant – i.e. by connecting two nodes in group of tightly interconnected nodes – will have a low relative resistance, whereas removing a link with high relative resistance would significantly reduce the connectivity between its endpoints. In [63], it was shown that sampling links proportional to their relative resistance yields statistically representative sparse samples of a graph, which is related to the concept of statistical load/leverage in numerical linear algebra [22].

To further quantify the notion of ‘link importance’ we introduce a well-known relation between relative resistances and random spanning trees – since the relative resistance of a link only depends on the connected component containing the link we will briefly assume the underlying graph to be connected. A *spanning tree*  $T$  of  $G$  is a connected subgraph which is a tree (i.e. has

---

<sup>2</sup>Formally, one can take the effective resistance to be infinite between nodes in different components.

<sup>3</sup>This is not standard terminology, but is introduced here because it has distinctly different properties and interpretations than the effective resistance  $\omega_{ij}$ . The name relative resistance follows from  $c_{ij}$  being a conductance (inverse resistance) in the context of electrical circuits, such that  $c_{ij}\omega_{ij}$  is the quotient between a link’s effective resistance and its ‘direct’ resistance as a resistor.

$n - 1$  links) and the set of all spanning trees is denoted by  $\mathcal{T}$ . A *random spanning tree*  $\mathbf{T}$  is a random element of  $\mathcal{T}$  with probability to equal any specific spanning tree  $T$  given by

$$\Pr[\mathbf{T} = T] = \frac{c(T)}{\sum_{T' \in \mathcal{T}} c(T')} \quad \text{with} \quad c(T) := \prod_{(i,j) \in \mathcal{L}(T)} c_{ij}$$

In other words, a random spanning tree is sampled proportional to  $c(T)$ , the product of its link weights. This relates to the relative resistance as, see also [46]:

**Theorem 2** ([41, 12]). *The relative resistance of a link equals the probability that this link is contained in a random spanning tree,  $c_{ij}\omega_{ij} = \Pr[(i, j) \in \mathbf{T}]$ .*

For graphs on multiple connected components, the same result holds in terms of random spanning forests which consist of a random spanning tree on each of the connected components independently. Theorem 2 is an important tool to study the relative resistance, and we will make use of the following properties (see Appendix A.1)

**Property 1** (relative resistance properties). *The relative resistance of a link  $(i, j)$  is bounded by  $0 < c_{ij}\omega_{ij} \leq 1$ , with equality in the upper bound if and only if it is a cut link. The sum over all relative resistances equals  $\sum_{i \sim j} c_{ij}\omega_{ij} = n - \beta$ , which is known as Foster’s Theorem.*

### 3 Introducing the resistance curvature

We will define two types of discrete curvature: a *scalar curvature* defined on the nodes of a graph as  $p : \mathcal{N} \rightarrow \mathbb{R}$  and a *Ricci curvature* defined on the links of a graph as  $\kappa : \mathcal{L} \rightarrow \mathbb{R}$ . We will refer to the nodal curvature simply as ‘resistance curvature’ and will use the slightly longer ‘link resistance curvature’ for the latter<sup>4</sup>.

**Definition 1** (resistance curvature). *The resistance curvature is defined as*

$$p_i := 1 - \frac{1}{2} \sum_{j \sim i} \omega_{ij} c_{ij} \quad \text{for any node } i \in \mathcal{N}. \quad (2)$$

The resistance curvature is a node function, but instead of writing  $p(i)$  we will mostly write  $p_i$  for a node  $i$  and use the  $n \times 1$  vector  $\mathbf{p} = (p_1, \dots, p_n)^T$  containing all resistance curvatures<sup>5</sup>. The definition of  $p$  appeared before in [76, 6], and [18, Proposition I.2] presents a number of alternative expressions for  $p$ , but to our knowledge the connection to curvature has not yet been made. We furthermore remark that while the resistance curvature is defined *locally* as a sum over the relative resistances of the incident links, the relative resistance and thus  $p_i$  depend on the structure of the whole graph in general. Thanks to efficient algorithms for Laplacian systems however, the resistance curvature can still be calculated efficiently, as discussed at the end of this section.

Following Property 1 for the relative resistance, we can find some first basic results on the node resistance curvature (see Appendix A.2):

**Property 2.** *The resistance curvature is bounded by  $1 - d_i/2 \leq p_i \leq 1/2$ , with equality in the lower bound if and only if all links  $j \sim i$  are cut links. The sum over all resistance curvatures equals  $\sum_{i \in \mathcal{N}} p_i = \beta$ .*

<sup>4</sup>While finishing the manuscript, we found that the name “effective resistance curvature” was introduced in [31] for a different notion of curvature derived from effective resistances.

<sup>5</sup>To be fully consistent, we can assume a bijection between  $\mathcal{N}$  and the integers  $[n] = 1, \dots, n$  such that we can index the nodes of  $G$  both as  $i \in \mathcal{N}$  or as  $1 \leq i \leq n$ .

In tree graphs, every link is a cut link and thus Property 2 implies that the non-leaf nodes in a tree have nonpositive curvature. For path graphs – which are tree graphs with nodes of degree 1 and 2 – we find that the two end nodes have resistance curvature  $1/2$  while all other nodes have zero curvature. The bounds for  $p$  in Property 2 thus produce some examples where negative and zero curvature happen generically, i.e. in tree and path graphs. To add an example of positive curvature, we can consider the cycle graph. By virtue of the rotational symmetry of the cycle graph, all nodes are indistinguishable and should thus have the same resistance curvature; by  $\sum p_i = 1$  this then implies that the resistance curvature is positive and equal to  $p_i = 1/n$  for all nodes in the  $n$ -cycle graph (see Appendix B for more detail). These three examples are treated in further detail at the end of this section.

Starting from the (scalar) node resistance curvature we now introduce the (Ricci) link resistance curvature:

**Definition 2** (link resistance curvature). *The link resistance curvature is defined as*

$$\kappa_{ij} := \frac{2(p_i + p_j)}{\omega_{ij}} \text{ for any link } (i, j) \in \mathcal{L}. \quad (3)$$

The link resistance curvature equals the sum of the (nodal) resistance curvature of its end nodes, divided by their effective resistance. Consequently, calculating the link resistance curvature is straightforward once  $p$  is known, and when  $p_i$  and  $p_j$  have the same sign this immediately determines the sign of  $\kappa_{ij}$  as well. Tree, path and cycle graphs can thus serve as a first example of graphs with links of negative/zero/positive link curvature.

Following the bounds for  $p$  we find the following bounds for  $\kappa$  (see Appendix A.3):

**Property 3.** *The link resistance curvature is bounded by  $c_{ij}(4 - d_i - d_j) \leq \kappa_{ij} \leq 2/\omega_{ij}$ , with equality in the lower bound if and only if all incident links to  $i$  and  $j$  are cut links.*

Both  $p$  and  $\kappa$  can be calculated efficiently. While computing effective resistances based on definition (1) requires a costly matrix inversion, the specific structure of Laplacian matrices can be exploited to approximate the effective resistance of any link in the graph with accuracy  $(1 - \epsilon)$  in time  $O(m \log(c_{\max}/c_{\min})/\epsilon^2)$ , i.e. basically in linear time in the number of links [63, 69]. As a consequence,  $p$  and  $\kappa$  can be calculated efficiently.

### 3.1 Examples

We discuss a few examples to support the introduced definitions; we describe some classes of graphs where positive, zero and negative curvature occurs generically and show some results for Erdős-Rényi random graphs. Figures 2 and 3 illustrate the examples.

**Example 1 (tree graphs)** As introduced, a tree graph is a connected graph with  $m = n - 1$  links. Since every link in a tree graph is a cut link, the bounds in Properties 1-3 hold with equality, and we find that

$$c_{ij}\omega_{ij} = 1 \quad p_i = 1 - \frac{d_i}{2} \quad \kappa_{ij} = c_{ij}(4 - d_i - d_j).$$

for all nodes  $i$  and links  $(i, j)$ . In other words, except for the leaf nodes and the links connected to them, all nodes and links have nonpositive node/link resistance curvature.

**Example 2 (path graphs)** A path graph is a tree with two leaf nodes forming the ends of the path, and all other nodes having degree two. Following the result for tree graphs we find that

$$\begin{cases} p_i = \frac{1}{2} \text{ at the end nodes} \\ p_i = 0 \text{ otherwise} \end{cases} \quad \begin{cases} \kappa_{ij} = c_{ij} \text{ if } i \text{ or } j \text{ is an end node} \\ \kappa_{ij} = 0 \text{ otherwise} \end{cases}$$

In other words, except for the end nodes and the links connected to them, all nodes and links have zero curvature. The case of a 2-node path is slightly different as we get  $\kappa_{ij} = 2c_{ij}$ .

**Example 3 (cycle graphs)** As noted before, the symmetries of a graph can have implications for the resistance curvature. In Appendix B we show that the relevant notion of symmetry is node (link) *transitivity* which says that any node (link) can be mapped onto any other node (link) by some structure-preserving map, i.e. an automorphism. One example of a node and link transitive graph is the cycle graph, for which the node and link resistance curvatures equal (see Appendix B):

$$c\omega_{ij} = \frac{n-1}{n} \quad p_i = \frac{1}{n} \quad \kappa_{ij} = \frac{4c}{n-1}$$

for all nodes  $i$  and links  $(i, j)$  and constant link weight  $c$ . In other words, all nodes and links are positively curved. Some more examples of transitive graphs will be discussed in Section 4.1. Figure 2 shows an example of tree, path and cycle graphs and their curvatures.

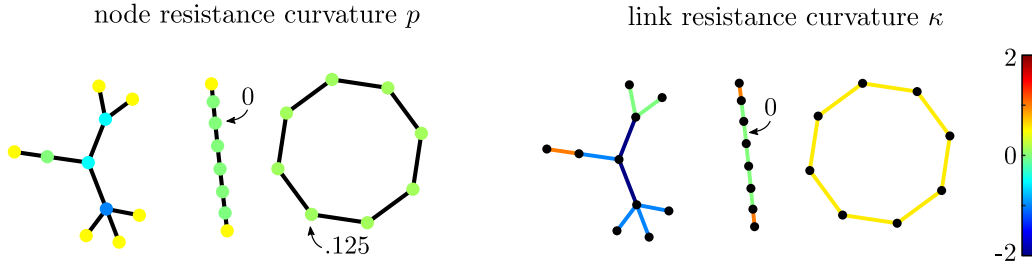


Figure 2: The node and link resistance curvatures in a tree, path and cycle graph (left to right).

**Example 4 (Erdős-Rényi random graph)** An *Erdős-Rényi* (ER) graph is a random graph where every pair of nodes is connected with probability  $\rho$ . Figure 3 shows how the mean link curvature  $\frac{1}{m} \sum_{i \sim j} \kappa_{ij}$  evolves in these random graphs as a function of the connection probability (density)  $\rho$ . An intuitive explanation for the observed evolution is as follows: ER graphs with very small  $\rho$  typically consist of a collection of 2-paths and disconnected nodes (graph *A* in Figure 3) with a mean link curvature of +2 since  $\kappa_{ij} = 2$  for a 2-path. For increasing  $\rho$ , the ER graph will be a collection of trees or locally tree-like components (graphs *B, C*) resulting in a decreasing  $\kappa$ , and eventually the graph will become a dense connected graph (graph *D*) with increasing  $\kappa$  until it reaches mean link curvature +2 for the complete graph at  $\rho = 1$ . In Section 4.3 we treat Euclidean random graphs as another example of random graphs.

## 4 Curvature properties of $p$ and $\kappa$

In the previous section, we introduced the node and link resistance curvature based on effective (and relative) resistances. However, so far the only hint towards an interpretation of  $p$  and  $\kappa$  as notions of discrete curvature were some examples of graphs with negative/zero/positive curvature. In this section, we present three arguments that further evidence this interpretation. A brief summary of the arguments is given below and each argument is then presented in more detail in the following subsections. While these arguments do not constitute a ‘proof’ that  $p$  is a discrete scalar curvature and  $\kappa$  a discrete Ricci curvature, we believe that they make a strong case and hope that this will provide a good starting point for further research. The arguments can be summarized as follows:

- (1) The resistance curvatures are constant and of the correct sign for a number of graphs associated to **constant curvature spaces**. We show this for infinite regular lattices (0), infinite regular trees ( $< 0$ ) and platonic graphs as regular tilings of the sphere ( $> 0$ ).

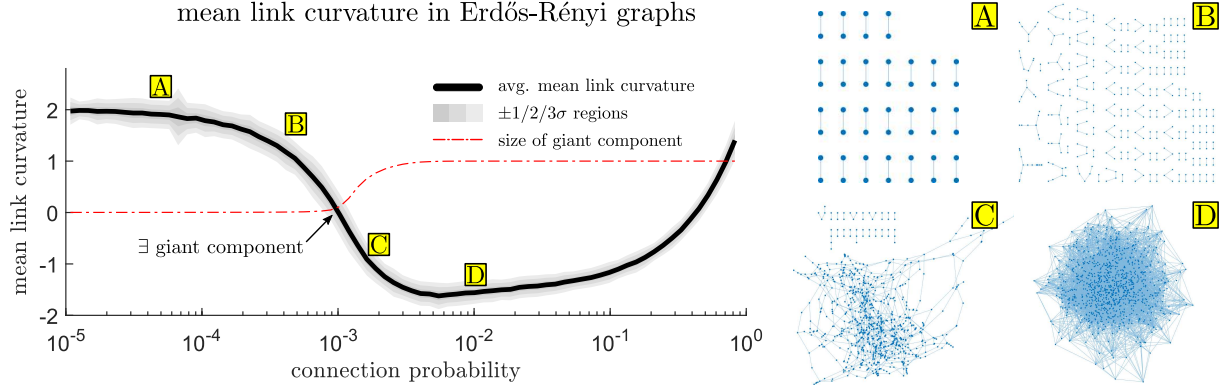


Figure 3: *Evolution of the mean link resistance curvature in Erdős-Rényi (ER) graphs for different connection probabilities (densities)  $\rho$ . We select  $N_\rho = 10^4$  connection probabilities  $\log_{10}(\rho) \in [-5, -0.05]$  uniformly at random, construct an ER random graph on  $n = 10^3$  nodes for each probability and calculate the mean link resistance curvature  $\frac{1}{m} \sum_{j \sim i} \kappa_{ij}$  in each graph. **The left figure** shows the sample average of the mean link resistance curvature, with graph samples binned together according to their connection probabilities ( $N_{\text{bins}} = 75$ ), and  $\pm 1/2/3$  standard deviations around the average. In red, the size of the giant component ( $= \text{no. nodes in largest component}/n$ ) is plotted, again averaged according to the bins; we remark that the appearance of a giant component around  $(n-1)\rho = 1$  coincides with the mean link curvature crossing zero. **The right figure** shows four ER graphs (A-D) with different connection probabilities to illustrate the evolution from a collection of many small tree-like components (A,B) for small  $\rho$  to the emergence of a larger locally tree-like component (C) and finally, a dense connected graph (D) as  $\rho$  further increases – components consisting of single nodes are omitted for clarity*

- (2) The resistance curvatures are **related to established notions of discrete curvature** on graphs. We show that the node resistance curvature is related to combinatorial curvature and that the link resistance curvature satisfies ‘Forman curvature  $\leq$  link resistance curvature  $\leq$  Ollivier curvature’.
- (3) We show numerical and theoretical evidence that the node resistance curvature retrieves **zero curvature in Euclidean random graphs**.

#### 4.1 Constant curvature graphs

**Positive curvature (platonic graphs)** Platonic graphs are the graph skeletons of the platonic solids (tetrahedron, cube, octahedron, dodecahedron, icosahedron), which are regular tilings of the 2-sphere  $\mathbb{S}^2$ . By transitivity of these graphs, we know from Appendix B that the resistance curvatures will be constant and positive, equal to  $p_i = 1/n$  and  $\kappa_{ij} = 2\rho$ , where  $\rho = m/\binom{n}{2}$  is the link density. This is in correspondence with the constant positive curvature of  $\mathbb{S}^2$ .

**Zero curvature (infinite lattice)** The rectangular/triangular/hexagonal lattices are infinite graphs that correspond to (the graph skeleton of) the regular tilings of the Euclidean plane, and can thus be embedded isometrically in  $\mathbb{R}^2$ . The effective resistance in these lattices has been studied extensively and it was shown that the relative resistance of all links is equal to  $2/d$ , with  $d$  the degree of the respective lattice [21, 66, 25]. Consequently, the lattice graphs have constant zero resistance curvatures  $p_i = 0$  and  $\kappa_{ij} = 0$ , in correspondence with the zero curvature of  $\mathbb{R}^2$ .

**Negative curvature (infinite regular tree)** The infinite regular tree or Bethe lattice [50] corresponds to a regular tiling of the hyperbolic plane  $\mathbb{H}^2$ . Like all trees, the relative resistance of every link is equal to one which means that these graphs have negative resistance curvatures  $p_i = 1 - d/2$  and  $\kappa_{ij} = 2c(2 - d)$  when degree  $d > 2$ , in correspondence with the constant negative curvature of  $\mathbb{H}^2$ .



Some examples of these constant curvature graphs are shown in Figure 1. We remark that the correct curvature in regular tilings is not always reproduced correctly by the established notions of discrete curvature. As noted in [40] for instance, the hexagonal lattice is often assigned a negative curvature because it is locally tree-like.

## 4.2 Relation to other discrete curvatures

As a second argument, we show that the node resistance curvature  $p$  is related to combinatorial curvature (through random spanning trees) and that the link resistance curvature is related to Ollivier-Ricci and Forman-Ricci curvature (through tight two-sided bounds).

### 4.2.1 Node resistance curvature and combinatorial curvature

Combinatorial curvature [39, 32] measures discrete curvature for graphs embedded in the plane (or other surfaces), i.e. with the nodes and links drawn in the plane such that the links only intersect at their endpoints. These drawings partition the plane into *faces* which are connected regions of the plane bordered by links that form a cycle in the graph. The combinatorial curvature is then defined as [39]

$$p_i^{(co)} := 1 - \frac{d_i}{2} + \sum_{\text{face } f \ni i} \frac{1}{d_f},$$

where  $f \ni i$  are the faces that contain node  $i$  in their boundary. For tree graphs, only a single unbounded face exists which does not contribute to the combinatorial curvature such that every node in a tree graph has combinatorial curvature  $1 - d_i/2$  equal to the node resistance curvature. Following the connection between relative resistances and random spanning trees, we moreover find that the resistance curvature of a node  $i$  in a general graph equals the expected combinatorial curvature of  $i$  in a random spanning tree; in other words (see Appendix C.1):

$$p_i = \mathbb{E}[p_i^{(co)}(\mathbf{T})] \text{ with random spanning tree } \mathbf{T}. \quad (4)$$

### 4.2.2 Resistance curvature and Ollivier-Ricci curvature

Yann Ollivier [55] introduced a notion of curvature for metric spaces with an associated Markov chain. This notion of discrete curvature can readily be applied to graphs where the shortest path or geodesic distance is a natural metric  $d : \mathcal{N} \times \mathcal{N} \rightarrow \mathbb{R}$ , and with lazy random walks taking the role of a Markov chain<sup>6</sup>  $\mu_t$ . For every node  $i$ , the Markov chain determines a function  $\mu_{t,i} : \mathcal{N} \rightarrow [0, 1]$  on the nodes, which gives the probability to find the random walker at a node one step after being at  $i$  (see later for some examples). This function can be thought of as a ‘ball’ around  $i$  in the graph. The metric  $d$  can be lifted to provide a notion of distance between these balls by making use of the 1-Wasserstein distance  $W_1$ :

$$W_1(\mu_{t,i}, \mu_{t,j}) := \min_P \text{tr}(PD),$$

where the minimum is taken over all nonnegative  $n \times n$  matrices  $P$  with ‘marginals’  $\sum_j (P)_{xj} = \mu_{t,i}(x)$  and  $\sum_i (P)_{ix} = \mu_{t,j}(x)$  and where matrix  $(D)_{ij} = d(i, j)$  is the *distance matrix* of the graph. *Ollivier-Ricci* (OR) curvature measures how much the *direct distance*  $d(i, j)$  between two nodes differs from the *distance between balls* around these nodes  $W_1(\mu_{t,i}, \mu_{t,j})$  as a generalization

---

<sup>6</sup>The subscript ‘ $t$ ’ of the Markov chain is the *laziness parameter* of the random walk and should not be confused with the ‘Markov time’ of a continuous-time Markov chain which is often denoted by  $t$  as well. For a given random walk with transition probabilities  $T_{ij} = \Pr[j \text{ at step } k+1 | i \text{ at step } k]$ , the lazy random walk has transition probabilities  $T'_{ij} = (1-t)I + tT_{ij}$ , i.e. with probability  $(1-t)$  to stay at the same node each step.

of continuous Ricci curvature to the data  $(\mathcal{N}, d, \mu_t)$ . Lin, Lu and Yau further modified Ollivier's definition as a limit for shrinking balls as [45]

$$\kappa_{ij}^{(OR)} := \lim_{t \rightarrow 0} \frac{1}{t} \left( 1 - \frac{W_1(\mu_{t,i}, \mu_{t,j})}{d(i, j)} \right).$$

For  $t \rightarrow 0$ , the distances  $W_1$  and  $d$  will converge and OR curvature thus measures how much they differ in the first order in  $t$ . If the distance between the balls is larger than the direct distance between the points then  $\kappa^{(OR)}$  will be negative, and the other way around for positive curvature.

One choice for Markov chain  $\mu_t$  is the *lazy random walk*

$$\mu_{t,i}(j) = \begin{cases} 1 - tk_i & \text{if } i = j \\ c_{ij}t & \text{if } j \sim i \\ 0 & \text{else} \end{cases} \quad \text{for } 0 \leq t \leq k_{\max}^{-1}$$

which can be defined compactly as the vector  $\mu_{t,i} = (I - Qt)\mathbf{e}_i$ , where  $I$  is the identity matrix<sup>7</sup>. While the OR curvature has been studied with respect to this Markov chain and the geodesic distance, we have not found it being used in conjunction with the effective resistance distance. We find that OR curvature with respect to the data  $(\mathcal{N}, \omega, (I - Qt))$  relates to the link resistance curvature as (see Appendix C.2):

**Proposition 1.** *The Ollivier-Ricci curvature with respect to resistance distance and the lazy random walk is lower-bounded by the resistance curvature as  $\kappa_{ij}^{(OR)} \geq \kappa_{ij}$ , with equality if  $(i, j)$  is a cut link.*

In tree graphs, all links are cut links and the link resistance curvature will thus correspond to the OR curvature throughout the graph. Furthermore, we note that the resistance distance is equal to the geodesic distance in trees.

An alternative Markov chain that is used more often is the normalized lazy random walk, defined by  $\mu_{t,i} = (I - Q \text{diag}(\mathbf{k})^{-1}t)\mathbf{e}_i$  where  $\text{diag}(\mathbf{k})$  is the diagonal matrix with the weighted degrees on its diagonal [45, 51]. Similar to the standard lazy random walk, we find the bound

$$\kappa_{ij}^{(LLY)} \geq \frac{2(p_i/k_i + p_j/k_j)}{\omega_{ij}} \quad (5)$$

which suggests a degree-normalized version of the link resistance curvature. The superscript LLY refers to the authors Lin, Lu and Yau of [45] where this variant of OR curvature was first considered.

#### 4.2.3 Resistance curvature and Forman-Ricci curvature

In [26], Robin Forman introduced a new notion of curvature for CW complexes, a class of discrete/combinatorial spaces that includes graphs. This so-called Forman-Ricci (FR) curvature is defined by generalizing the definition of the classical Ricci curvature in terms of the Bochner Laplacian of a manifold to a definition for discrete spaces based on an analogous Bochner Laplacian on these spaces, see also [38]. The FR curvature is expressed in terms of *local* combinatorial data around a considered point, and Sreejith et al. [64] translated Forman's general definition to graphs as

$$\kappa_{ij}^{(FR)} = 2w_i \left( 1 - \frac{1}{2} \sum_{k \sim i} \sqrt{\frac{w_{ij}}{w_{ik}}} \right) + 2w_j \left( 1 - \frac{1}{2} \sum_{k \sim j} \sqrt{\frac{w_{ij}}{w_{jk}}} \right) \quad (6)$$

---

<sup>7</sup>For small  $t$ , the same random walk is obtained from the continuous-time Markov chain  $\tilde{\mu}_{t,i} = e^{-Qt}\mathbf{e}_i$  which was also used in [30].

where  $w_*$  are some nonzero weights associated to the nodes and links of the graph. Expression (6) clearly resembles the definition of  $\kappa$  in terms of the node resistance curvature and indeed, choosing unit weights yields the following relation (see Appendix C.3):

**Proposition 2.** *The Forman-Ricci curvature with respect to unit weights is upper-bounded by the link resistance curvature as  $c_{ij}\kappa_{ij}^{(FR)} \leq \kappa_{ij}$ , with equality if and only if  $(i, j)$  is a cut link.*

*Remark:* If we choose the inverse degree as node weights  $w_i = 1/k_i$  and consider graphs with  $c = 1$ , then we find the bound  $\kappa_{ij}^{(FR)} \leq 2(p_i/k_i + p_j/k_j)/\omega_{ij}$  which again features the degree-normalized version of the link resistance curvature as in (5).

**Summary** The relation between the link resistance curvature and Forman and Ollivier-Ricci curvature can be summarized by the two-sided bound

$$\kappa_{ij}^{(OR)} \geq \kappa_{ij} \geq c_{ij}\kappa_{ij}^{(FR)} \text{ with equality for cut links,}$$

where we stress that these are OR and FR curvatures with respect to particular data:  $\omega$  as metric for OR and  $w = 1$  as weight for FR. Apart from being an argument for the interpretation of the link resistance curvature as a discrete curvature, this result is relevant in the context of other works that investigate the relation between both curvatures [38, 65, 59].

### 4.3 Resistance curvature for Euclidean random graphs

A natural question for discrete curvatures is whether they converge to continuous curvature on discrete structures that represent finer and finer discretizations of some continuous space. For instance, van der Hoorn et al. [68] recently proved convergence of Ollivier-Ricci curvature to Ricci curvature in the continuum limit of random geometric graphs sampled from Riemannian manifolds. Here, as our third argument, we consider Euclidean random graphs and find numerical and theoretical evidence that the resistance curvature of these graphs retrieves the underlying zero curvature of the Euclidean plane.

A Euclidean random graph (ERG) is a random graph constructed on some domain  $\mathbb{D} \subseteq \mathbb{R}^2$  in the plane from which points are sampled uniformly at random by a Poisson point process with a homogeneous rate  $\lambda$ ; the expected number of points is equal to  $N = \lambda \text{Area}(\mathbb{D})$  so we may equivalently fix a desired  $N$ . These points are then taken as the nodes of a graph and pairs of nodes are linked if they lie within a certain connection radius (distance)  $r$  from each other. All together, a Euclidean random graph model or ensemble can thus be parametrized by  $(\mathbb{D}, N, r)$ . See [56] for more information on ERGs and their properties and Figure 4 for an illustration of their construction and some examples.

To simplify the setup for further analysis, we consider ERGs on the disc  $\mathbb{D} = \{x \in \mathbb{R}^2 : \|x\| \leq R\}$  of radius  $R$ , such that nodes at the same radial distance  $D_i$  from the boundary are statistically equivalent, and the effective parameters reduce to  $(R/r, N)$ .

As a first numerical analysis, Figure 4 shows the resistance curvatures in a Euclidean random graph on the disc with  $R/r = 4$  and  $N = 2 \cdot 10^3$  nodes. Near the center of the disc, which we call the *bulk* of the graph, we clearly observe that the curvatures are close to zero, while moving towards the boundary the resistance curvature becomes first negative and then positive at the boundary. Figure 5 shows this result in more detail: the mean and standard deviations of  $p_i$  are plotted with respect to  $D_i/r$  with data aggregated over 100 samples of an ERG with  $R/r = 5$  and  $N = 5 \cdot 10^3$ . The main observation in Figure 5 is again that  $p_i$  is close to zero in the bulk – moreover, it appears to be a zero-mean random variable – and becomes negative and then positive when moving closer to the boundary.

We now develop a model for the resistance curvature in Euclidean random graphs that partly explains these observations. While a full understanding of the relative resistance in ERGs is

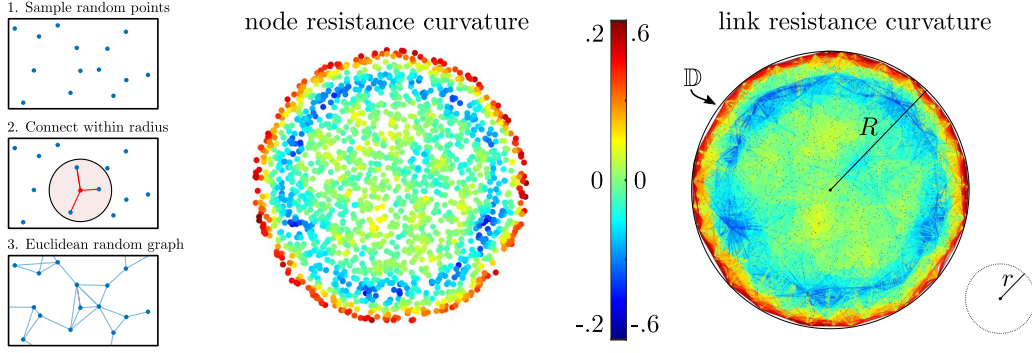


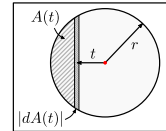
Figure 4: **The left panels** illustrate the construction of a Euclidean random graph (ERG): points are randomly sampled from a domain  $\mathbb{D} \subseteq \mathbb{R}^2$  and connected if they lie within a certain connection radius  $r$ . **The right figure** shows the resistance curvature calculated in an ERG on a disc with radius  $R/r = 4$  and expected number of nodes  $N = 2.10^3$ , with red/green/blue indicating positive/zero/negative values. Visually, both the node and link resistance curvatures are close to zero near the center of the disc but become negative and then positive going closer to the boundary. More detailed experimental results are shown in Figure 5 and the origin of the boundary effect is explained in the main text and Appendix D.

lacking, in particular concerning dependencies between the relative resistance of different links, we find that the numerical observations in Figures 4 and 5 can be explained in great detail using a simple heuristic for the effective resistance. In [71, 72], von Luxburg et al. showed that in ERGs with increasing number of nodes, the effective resistance between any pair of nodes  $i, j$  converges to the sum of their inverse degrees  $d_i^{-1} + d_j^{-1}$ . While the degree of a node depends on the specific random graph realization, we know by properties of Poisson sampling that the *expected degree* of a given node  $i$  is determined by the area of overlap between the domain and an  $r$ -radius disc centered at  $i$ , in other words  $\mathbb{E}(d_i) = \lambda S(i)$  where  $S(i) := \text{Area}(\{x \in \mathbb{D} : \|x - i\| \leq r\})$ , with expectation over the random graph ensemble. Combining these two results, we propose the following heuristic  $\hat{\omega}$  for the effective resistance in ERGs:

$$\hat{\omega}_{ij} := \frac{1}{\lambda S(i)} + \frac{1}{\lambda S(j)} \text{ for all links } i \sim j. \quad (7)$$

Importantly, this reduces the effective resistance of a link to a purely *geometric and local* quantity that is only determined by how the  $r$ -radius region around the link overlaps with the domain  $\mathbb{D}$ . In Appendix D, we show that this heuristic combined with the assumption that  $r \ll R$  allows to calculate the expected resistance curvature  $\hat{p}$  as a function of the distance to the boundary  $D$  as

$$\mathbb{E}(\hat{p}(D)) = \frac{1}{2} \left( 1 - \int_{t=-r}^{\min(D,r)} \frac{|dA(t)|}{A(\max(-r, t - D))} \right) \quad (8)$$



where  $A(t)$  is the area of a circular segment at height  $t$  and  $|dA(t)|$  the change of segment size – as illustrated in the figure on the right – and with expectation taken over the ERG ensemble. While we were not able to find a general closed-form expression for the integral in (8), the expression can be evaluated numerically and is shown in Figure 5 by the red line. Importantly, Figure 5 shows that formula (8) matches very well with the experimentally observed resistance curvatures (the black line). This agreement suggests that our heuristic captures the main mechanisms behind the convergence of resistance curvature in Euclidean random graphs.

Due to the appearance of *min* and *max* operations, expression (8) is a piecewise function of the boundary distance  $D$ . In Appendix D, we show that there are three possible regimes for  $D$

as a result of the different local geometries around a node, i.e. how much of the connection discs around the node and its neighbours overlap with the domain (see also Figure 5). We find the following cases: (A) the *boundary regime*  $D \leq r$  where nodes as well as some of their neighbours are influenced by the boundary, (B) the *near-boundary regime*  $r \leq D \leq 2r$  where nodes are not influenced directly by the boundary (i.e. no overlap between the connection disc and the boundary), but some of its neighbours are, and (C) the *bulk regime*  $D \geq 2r$  where nodes are at least two connection radii away from the boundary such that the nodes nor any of their neighbours are influenced by the boundary. Most importantly, in the bulk regime expression (8) simplifies to  $\mathbb{E}(\hat{p}(D)) = 0$  which means that we have zero node resistance curvature  $\hat{p}$  in expectation in the bulk of ERGs. In the limit of  $r/R \rightarrow 0$ , this bulk regime will take up all but a vanishing fraction of the domain and almost all nodes will thus have zero expected resistance curvature. We remark that the derivation for expression (8) in Appendix D is independent of the specific shape of the domain  $\mathbb{D}$ , i.e. it need not be a disc, and that for ERGs in higher dimensions  $A(t)$  would simply be replaced by the volume of a higher-dimensional spherical cap.

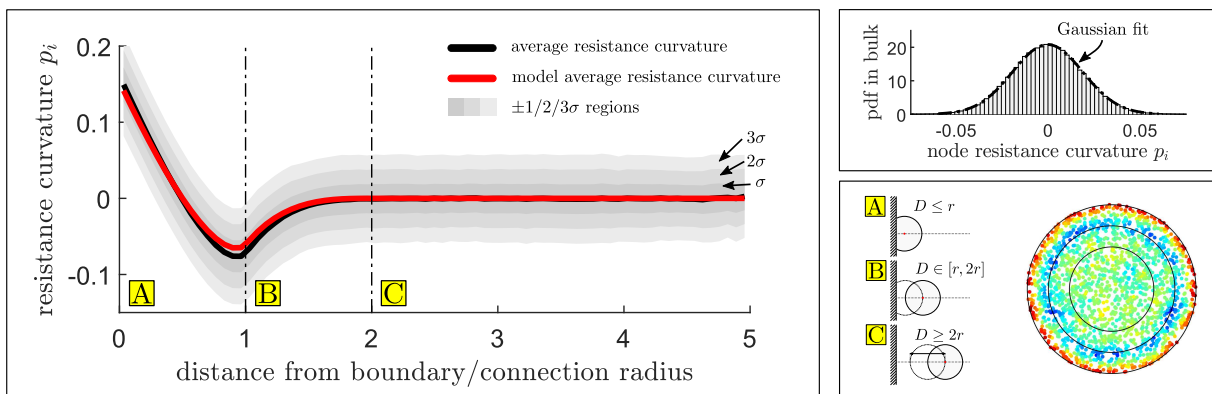


Figure 5: **Left panel:** We sample 100 graphs from an ERG on a disc with  $R/r = 5$ ,  $N = 5.10^3$  and calculate the node resistance curvature  $p_i$  for all nodes. The plot shows the mean and variation around the mean of these curvatures (vertical axis) as a function of the distance from the boundary divided by the connection radius  $D_i/r$  (horizontal axis). The red line shows the heuristic  $\mathbb{E}(\hat{p}(D))$  (expression (8)) which is in close correspondence to the black line, the experimental approximation for  $\mathbb{E}(p(D))$ . The boundary (A), near-boundary (B) and bulk regime (C) are delineated by vertical black lines and the **bottom right** panel illustrates how these different regimes correspond to different local geometries of the nodes (see also Appendix D). The **top right** panel shows the distribution of  $p_i$  for nodes in the bulk regime and the maximum likelihood Gaussian fit of this distribution; the good correspondence of this fit suggests that  $p_i$  could be a zero-mean Gaussian random variable in the bulk.

## 5 Discrete Ricci flow

Ricci flow is an important concept associated to curvature in differential geometry [14]. Intuitively, the Ricci flow describes a curvature-dependent evolution of the metric of a Riemannian manifold, where the metric decreases in directions of positive curvature while increasing in directions of negative curvature. The overall effect of this flow is that the curvature is ‘smoothed out’ and for this reason, the Ricci flow is also thought of as a form of nonlinear heat equation for the metric. Due to its importance in the continuous setting, there have been several proposals to define a Ricci flow in the case of discrete curvatures, with various applications: Jin et al. [35] define a Ricci flow for meshes in computer graphics, Ni et al. [54] use a Ricci flow inspired evolution of networks for community detection and network alignment and Weber et al. considered Ricci flows related to the Forman Ricci curvature [73]. Recently, Bai et al. studied

a Ricci flow based on the Lin-Yu-Yau curvature [4]. Here, we show that there is a natural Ricci flow associated to the resistance curvature with promising features.

### 5.1 Resistance Ricci flow

Ollivier proposed in [55, Problem N] to look at the differential equation  $\frac{d}{dt}d(i, j) = -\kappa_{ij}^{(OR)}d(i, j)$  as a discrete version of the Ricci flow. If we introduce the link resistance curvature  $\kappa_{ij}$  and resistance distance  $d(i, j) = \omega_{ij}$  in this expression, we find

$$\frac{d\omega_{ij}}{dt} = -2(p_i + p_j) \text{ for all } i \neq j \text{ in the same component} \quad (9)$$

which we call the *resistance Ricci flow*; since  $\omega$  is metric, we implicitly have  $d\omega_{ii}/dt = 0$ . Ideally, equation (9) would describe the evolution of a resistance matrix  $(\Omega(t))_{ij} = \omega_{ij}(t)$  for all  $t > 0$  and starting from any initial resistance matrix  $\Omega_0 := \Omega(0)$ . Unfortunately however,  $\Omega(t)$  is in general not guaranteed to be a resistance matrix as the flow can result in graphs with negative and diverging link weights in finite time as we show below. Nonetheless, we find that the resistance Ricci flow satisfies a number of interesting properties. As the flow (9) affects each connected component independently, we will assume  $G$  to be connected in the rest of this section.

If  $S$  is a state space (e.g. a vector space) and  $P : S \rightarrow \mathbb{R}$  a potential defined on this state space, then the evolution  $ds/dt = -\nabla P$  for a flow  $s(t) \in S$ , assuming that it is well-defined, is called a *gradient flow*. This name reflects that the resulting flow follows the direction of steepest descent of the potential  $P$ , as given by the negative gradient. As a first result, we find that the resistance Ricci flow is a gradient flow (see Appendix E):

**Proposition 3.** *The resistance Ricci flow (9) is a gradient flow of the potential  $\text{tr}(\frac{1}{2}\Omega Q\Omega)$  defined on symmetric zero-diagonal matrices  $\Omega$ , as*

$$\frac{d\Omega}{dt} = -\nabla_{\Omega} \text{tr} \left( \frac{1}{2}\Omega Q\Omega \right), \quad (10)$$

*Remark:* The gradient  $\nabla_{\Omega}$  is defined on the state space of symmetric zero-diagonal matrices, such that the flow  $\Omega(t)$  remains symmetric and with zero-diagonal; see Appendix E for further details.

The gradient form (10) relates the resistance Ricci flow to the classical diffusion equation for a density  $\mathbf{x}$  in  $\mathbb{R}^n$ , which is a gradient flow for the potential  $\text{tr}(\frac{1}{2}\mathbf{x}^T Q \mathbf{x})$ . Expression (10) could have practical implications for the resistance Ricci flow: since the potential is a decreasing function of time for gradient dynamics as  $d\text{tr}(\frac{1}{2}\Omega Q\Omega)/dt < 0$ , this could be a starting point to study convergence of the resistance Ricci flow.

In Appendix E, we furthermore show that the potential can be rewritten as  $\text{tr}(\frac{1}{2}\Omega Q\Omega) = 2n\sigma^2$  where  $\sigma^2 = \frac{1}{2}p^T \Omega p$  is a graph invariant that appears in several contexts in the study of effective resistances, see for instance [18] and [19, Appendix I]. The gradient expression (10) further adds to the theory of this invariant. As noted in [18], the number  $1/(2\sigma^2)$  also relates to the so-called *magnitude* (introduced in [44]) of the metric space  $(\mathcal{N}, \omega)$ ; this suggests to consider gradient flows of metric spaces with the magnitude as a potential function.

### 5.2 Flow of Laplacians

While expression (9) does not provide much insight into how the resistance Ricci flow affects the graph structure, we can also express the flow in terms of Laplacian matrices (see Appendix E):

**Proposition 4.** *The resistance Ricci flow (9) is equivalent to the following flow of Laplacian matrices:*

$$\frac{dQ}{dt} = 2Q \text{diag}(\mathbf{p})Q, \text{ for some initial Laplacian } Q(0) = Q_0. \quad (11)$$

Proposition 4 is remarkable since it shows that the resistance Ricci flow – which was defined based on the proposal of Ollivier – corresponds to a simple flow of Laplacian matrices. By considering the off-diagonal entries of expression (11), we can write the evolution of individual link weights as:

$$\frac{dc_{ij}}{dt} = -2 \sum_{\substack{k \sim i,j \\ k \neq i,j}} c_{ik} c_{kj} p_k + 2c_{ij} (k_i p_i + k_j p_j) \text{ for all } i \neq j, \quad (12)$$

where the equation for the diagonal ( $dk_i/dt$ ) follows from the conserved zero row sum. The change of link weights in the resistance Ricci flow is thus caused by two types of processes: there is one term for each shared neighbour  $k$  of  $i$  and  $j$  which can increase or decrease the link weight based on its resistance curvature  $p_k$ , and a second term based on the degrees and curvatures of  $i$  and  $j$ . Other works such as [2] have arrived at similar dynamical rules when modeling dynamic network structures, with a balance between positive link-reinforcing terms and competing link-decaying terms. As a possible variation on the resistance Ricci flow, one might consider the dynamics  $dQ/dt = 2Q \text{diag}(\mathbf{q})Q$  where  $q$  is some function on the nodes; for instance, if  $q$  depends on a process taking place on the graph such as in [2], this could model the codependent evolution of structure and processes. We now consider two examples of the resistance Ricci flow.

**Example 1 (node transitive graphs)** The node resistance curvature in node transitive graphs is constant and equal to  $p_i = 1/n$ . Furthermore, from (9) we find that  $d\omega_{ij}/dt = -2/n$  is equal for all pairs of nodes such that transitivity is conserved by the flow and thus  $p_i(t) = 1/n$  as long as this is well-defined. As a consequence, the resistance Ricci flow for node transitive graphs simplifies to  $dQ/dt = 2Q^2/n$ . Diagonalizing this equation and solving the differential equation  $dx/dt = 2x^2 \Rightarrow x(t) = x_0/(1 - 2tx_0)$  for each eigenvalue, we find the solution

$$Q(t) = \left[ I - \frac{2}{n} t Q_0 \right]^\dagger Q_0 \text{ for } t < \frac{n}{2\mu_{\max}(Q_0)}.$$

This flow *diverges in finite time* for  $t \rightarrow n/(2\mu_{\max})$ . The resistance Ricci flow for node transitive graphs is formally very similar to a matrix flow studied in [47] as a model for structural balance in social networks, which considers the differential equation  $dX/dt = X^2$  for a matrix  $X$ . The entries  $(X)_{ij}$  of this matrix represent pairwise affinities or rivalries, depending on the sign, and finite-time divergence was interpreted in the context of the model as the onset of a structurally balanced configuration of social relations.

**Example 2 (path graph)** All nodes in a path graph have zero node resistance curvature, except for the end nodes which have  $p = 1/2$ . From equation (12) for the evolution of link weights, we then find that the only change occurs for the end links, whose link weight evolves according to

$$\frac{dc}{dt} = c^2 \Rightarrow c(t) = \frac{c_0}{1 - c_0 t} \text{ for } t < \frac{1}{c_0},$$

and diverges to  $+\infty$  for  $t \rightarrow 1/c_0$ . While this result may seem pathological, we can interpret the ‘infinite affinity’ (which corresponds to  $\omega \rightarrow 0$ ) as merging the end node and its neighbour into a single node – this is a common operation in the theory of effective resistances. This analysis shows that the resistance Ricci flow of a path graph evolves by merging the end nodes of the path with their neighbours at  $t = 1/c_0$ , resulting in a path of decreasing length until just a single node remains.

Finally, we remark that the ‘degree-normalized’ link resistance curvature  $2(p_i/k_i + p_j/k_j)/\omega_{ij}$ , which naturally appears in correspondence with Ollivier and Forman Ricci curvature (see (5)), also has an associated Ricci flow  $d\omega_{ij}/dt = -2(p_i/k_i + p_j/k_j) \equiv dQ/dt = 2Q \text{diag}(\mathbf{p}/\mathbf{k})Q$ . Initial results suggest that this Ricci flow has additional interesting properties.

## 6 Conclusion

This article proposes new notions of discrete curvature based on the effective/relative resistance, and we introduce the *node resistance curvature*  $p : \mathcal{N} \rightarrow \mathbb{R}$  and *link resistance curvature*  $\kappa : \mathcal{L} \rightarrow \mathbb{R}$  in definitions (2) and (3) respectively. We provide a background on the effective and relative resistance, derive some basic theoretical results on  $p$  and  $\kappa$  and present a number of arguments that support the interpretation of  $p$  and  $\kappa$  as a curvature: they retrieve the correct (or expected) curvature for the discretization of some constant curvature spaces (§4.1), the resistance curvatures are related to established notions of discrete curvature, combinatorial, Ollivier-Ricci and Forman-Ricci curvature (§4.2) and we provide numerical and theoretical evidence that  $p$  retrieves zero curvature in expectation for Euclidean random graphs (§4.3). As an application, we show that the resistance curvatures have a natural associated Ricci flow and we discuss some of its properties.

While a full understanding of the relation to continuous curvature is still lacking, the resistance curvatures complement the existing study of discrete curvatures and, by their relation to the effective resistance with a rich theory, these new curvatures are a promising direction for further research in this area. In particular, the associated Ricci flow described in Section 5 seems to be more amenable to theoretical study than previously considered discrete Ricci flows.

Apart from the theoretical aspects, the resistance curvature may also prove to play an important role in the context of applications of discrete curvature. The resistance curvature assumes a space between the efficiently calculable but somewhat restrictively local Forman-Ricci curvature and the more integrative/expressive but computationally heavier Ollivier-Ricci curvature – the resistance curvatures  $p$  and  $\kappa$  combine local (in its definition) and global (in its dependence on the relative resistance) information on the graph structure and are efficient to calculate. Consequently, the resistance curvature may play a role in the further development of discrete curvature as a tool for network and data analysis.

Finally, we expect that our definitions may be translated from the setting of graphs to more general structures such as simplicial complexes, where (Hodge) Laplacians and effective resistances are also defined [43].

## References

- [1] E. Aamari, J. Kim, F. Chazal, B. Michel, A. Rinaldo, and L. Wasserman. Estimating the reach of a manifold, 2019. arXiv:1705.04565 [math.ST].
- [2] T. Aoki, K. Yawata, and T. Aoyagi. Self-organization of complex networks as a dynamical system. *Physical Review E*, 91(1):012908, 2015.
- [3] J. C. Baez and B. Fong. A compositional framework for passive linear networks. 2018. arXiv:1504.05625 [math.CT].
- [4] S. Bai, Y. Lin, L. Lu, Z. Wang, and S.-T. Yau. Ollivier Ricci-flow on weighted graphs. 2021. arXiv:2010.01802 [math.DG].
- [5] D. Bakry and M. Émery. Diffusions hypercontractives. In *Séminaire de Probabilités XIX 1983/84*, Lecture Notes in Mathematics, pages 177–206. Springer, Berlin, Heidelberg, 1985.
- [6] R. Bapat. Resistance matrix of a weighted graph. *MATCH Commun. Math. Comput. Chem.*, 50, 2004.
- [7] M. Berger. *Differential geometry: Manifolds, curves, and surfaces*. Graduate texts in mathematics ; 115. Springer-Verlag, New York, 1988.



- [8] N. Biggs. *Algebraic Graph Theory*. Cambridge tracts in mathematics ; 67. Cambridge University Press, Cambridge, 1974.
- [9] M. Boguna, I. Bonamassa, M. De Domenico, S. Havlin, D. Krioukov, and M. A. Serrano. Network geometry. *Nature Reviews Physics*, 3(2):114–135, 2021.
- [10] B. Bollobás. *Modern graph theory*. Graduate texts in mathematics ; 184. Springer, New York, 1998.
- [11] E. Bunch, J. Kline, D. Dickinson, S. Bhat, and G. Fung. Weighting vectors for machine learning: numerical harmonic analysis applied to boundary detection, 2021. arXiv:2106.00827 [cs.LG].
- [12] R. Burton and R. Pemantle. Local characteristics, entropy and limit theorems for spanning trees and domino tilings via transfer-impedances. *The Annals of probability*, 21(3):1329–1371, 1993.
- [13] G. Carlsson. Topology and data. *Bulletin (new series) of the American Mathematical Society*, 46(2):255–308, 2009.
- [14] B. Chow and D. Knopf. *The Ricci flow : An introduction*. Mathematical surveys and monographs ; v.110. American Mathematical Society, Providence, R.I. , 2004.
- [15] F. R. K. Chung. *Spectral graph theory*. American Mathematical Soc., Providence, US, 1997.
- [16] F. R. K. Chung and S.-T. Yau. Logarithmic Harnack inequalities. *Mathematical research letters*, 3(6):793–812, 1996.
- [17] R. R. Coifman and S. Lafon. Diffusion maps. *Applied and Computational Harmonic Analysis*, 21(1):5–30, 2006.
- [18] K. Devriendt. Effective resistance is more than distance: Laplacians, Simplices and the Schur complement. *Linear Algebra and its Applications*, 639:24–49, 2022.
- [19] K. Devriendt, S. Martin-Gutierrez, and R. Lambiotte. Variance and covariance of distributions on graphs. 2021. arXiv:2008.09155 [physics.soc-ph].
- [20] F. Dörfler, J. W. Simpson-Porco, and F. Bullo. Electrical networks and algebraic graph theory: Models, properties, and applications. *Proceedings of the IEEE*, 106(5):977–1005, 2018.
- [21] P. G. Doyle. Electric currents in infinite networks. 2007. arXiv:0703899 [math.PR].
- [22] P. Drineas and M. W. Mahoney. Effective resistances, statistical leverage, and applications to linear equation solving. 2010. arXiv:1005.3097 [cs.NA].
- [23] H. Federer. Curvature measures. *Transactions of the American Mathematical Society*, 93(3):418–491, 1959.
- [24] M. Fiedler. *Matrices and graphs in geometry*. Encyclopedia of mathematics and its applications ; 139. Cambridge University Press, Cambridge, 2011.
- [25] H. Flanders. Infinite networks: II—Resistance in an infinite grid. *Journal of mathematical analysis and applications*, 40(1):30–35, 1972.
- [26] R. Forman. Bochner’s method for cell complexes and combinatorial Ricci curvature. *Discrete & Computational Geometry*, 29(3):323–374, 2003.

- [27] A. Ghosh, S. Boyd, and A. Saberi. Minimizing effective resistance of a graph. *SIAM Review*, 50(1):37–66, 2008.
- [28] R. Ghrist. Barcodes: The persistent topology of data. *Bulletin (new series) of the American Mathematical Society*, 45(1):61–76, 2008.
- [29] C. D. Godsil and G. Royle. *Algebraic graph theory*. Graduate texts in mathematics ; 207. Springer, New York, 2001.
- [30] A. Gosztolai and A. Arnaudon. Unfolding the multiscale structure of networks with dynamical Ollivier-Ricci curvature. *Nature Communications*, 12(1):4561, 2021.
- [31] E. Grippo and E. A. Jonckheere. Effective resistance criterion for negative curvature: Application to congestion control. In *2016 IEEE Conference on Control Applications (CCA)*, pages 129–136, 2016.
- [32] M. Gromov. Hyperbolic groups. In *Essays in group theory*, pages 75–263. Springer, 1987.
- [33] A. D. Gvishiani and V. A. Gurvich. Metric and ultrametric spaces of resistances. *Russian Mathematical Surveys*, 42(6):235–236, 1987.
- [34] S. Hoory, N. Linial, and A. Wigderson. Expander graphs and their applications. *Bulletin (new series) of the American Mathematical Society*, 43(4):439–562, 2006.
- [35] M. Jin, J. Kim, F. Luo, and X. Gu. Discrete surface Ricci flow. *IEEE transactions on visualization and computer graphics*, 14(5):1030–1043, 2008.
- [36] E. Jonckheere, E. Grippo, and R. Banirazi. Curvature, entropy, congestion management and the power grid. In *2019 IEEE Conference on Control Technology and Applications (CCTA)*, pages 535–542, 2019.
- [37] J. Jost. *Riemannian geometry and geometric analysis*. Universitext. Springer, Berlin–New York, 1995.
- [38] J. Jost and F. Münch. Characterizations of Forman curvature. 2021. arXiv:2110.04554 [math.DG].
- [39] S. Kamtue. Combinatorial, Bakry-Émery, Ollivier’s Ricci curvature notions and their motivation from Riemannian geometry. 2018. arXiv:1803.08898 [math.CO].
- [40] M. Kempton, G. Lippner, and F. Münch. Large scale Ricci curvature on graphs. *Calculus of variations and partial differential equations*, 59(5), 2020.
- [41] G. Kirchhoff. Über die Auflösung der Gleichungen, auf welche man bei der Untersuchung der linearen Vertheilung galvanischer Ströme geführt wird. *Annalen der Physik*, 148(12):497–508, 1847.
- [42] D. J. Klein and M. Randić. Resistance distance. *Journal of Mathematical Chemistry*, 12(1):81–95, 1993.
- [43] W. Kook and K.-J. Lee. Simplicial networks and effective resistance. *Advances in Applied Mathematics*, C(100):71–86, 2018.
- [44] T. Leinster. The magnitude of metric spaces. *Documenta Mathematica*, 18:857–905, 2013.
- [45] Y. Lin, L. Lu, and S.-T. Yau. Ricci curvature of graphs. *Tohoku Mathematical Journal*, 63(4):605 – 627, 2011.

- [46] R. Lyons. Determinantal probability measures. *Publications Mathématiques de l'IHÉS*, 98:167–212, 2003.
- [47] S. A. Marvel, J. Kleinberg, R. D. Kleinberg, and S. H. Strogatz. Continuous-time model of structural balance. *Proceedings of the National Academy of Sciences*, 108(5):1771–1776, 2011.
- [48] R. Merris. Laplacian matrices of graphs: a survey. *Linear Algebra and its Applications*, 197-198:143 – 176, 1994.
- [49] B. Mohar, Y. Alavi, G. Chartrand, O. Oellermann, and A. Schwenk. The Laplacian spectrum of graphs. *Graph Theory, Combinatorics and Applications*, 2:871–898, 1991.
- [50] Mosseri, R. and Sadoc, J.F. The Bethe lattice : a regular tiling of the hyperbolic plane. *J. Physique Lett.*, 43(8):249–252, 1982.
- [51] F. Münch and R. K. Wojciechowski. Ollivier Ricci curvature for general graph Laplacians: Heat equation, Laplacian comparison, non-explosion and diameter bounds. 2017. arXiv:1712.00875 [math.DG].
- [52] K. A. Murgas, E. Saucan, and R. Sandhu. Quantifying cellular pluripotency and pathway robustness through Forman-Ricci curvature. 2021. bioRxiv doi: 10.1101/2021.10.03.462918.
- [53] C.-C. Ni, Y.-Y. Lin, J. Gao, X. D. Gu, and E. Saucan. Ricci curvature of the Internet topology. In *2015 IEEE Conference on Computer Communications (INFOCOM)*, pages 2758–2766. IEEE, 2015.
- [54] C.-C. Ni, Y.-Y. Lin, F. Luo, and J. Gao. Community detection on networks with Ricci flow. *Scientific Reports*, 9(1):9984, 2019.
- [55] Y. Ollivier. A survey of Ricci curvature for metric spaces and Markov chains. In *Probabilistic approach to geometry*, pages 343–381. Mathematical Society of Japan, 2010.
- [56] M. Penrose. *Random Geometric Graphs*. Oxford University Press, Oxford, 2003.
- [57] K. B. Petersen and M. S. Pedersen. The Matrix Cookbook, 2008. <http://www2.imm.dtu.dk/pubdb/p.php?3274>.
- [58] N. Peyerimhoff. Curvature notions on graphs Leeds summer school, 18-19 july 2019. <https://www.maths.dur.ac.uk/users/norbert.peyerimhoff/peyerimhoff-lecture-notes.pdf>.
- [59] A. Samal, R. P. Sreejith, J. Gu, S. Liu, E. Saucan, and J. Jost. Comparative analysis of two discretizations of Ricci curvature for complex networks. *Scientific Reports*, 8(1):8650, 2018.
- [60] E. Saucan, A. Samal, and J. Jost. A simple differential geometry for complex networks, 2020. arXiv:2004.11112 [math.MG].
- [61] J. Sia, E. Jonckheere, and P. Bogdan. Ollivier-Ricci curvature-based method to community detection in complex networks. *Scientific Reports*, 9(1):9800, 2019.
- [62] D. A. Spielman. Graphs, vectors, and matrices. *Notices of the American Mathematical Society*, pages 11–13, 2016.
- [63] D. A. Spielman and S.-H. Teng. Spectral sparsification of graphs. *SIAM Journal on Computing*, 40(4):981–1025, 2011.

- [64] R. P. Sreejith, K. Mohanraj, J. Jost, E. Saucan, and A. Samal. Forman curvature for complex networks. *Journal of Statistical Mechanics: Theory and Experiment*, 2016(6):063206, 2016.
- [65] P. Tee and C. A. Trugenberger. Enhanced Forman curvature and its relation to Ollivier curvature. *EPL (Europhysics Letters)*, 133(6):60006, 2021.
- [66] C. Thomassen. Resistances and currents in infinite electrical networks. *Journal of combinatorial theory. Series B*, 49(1):87–102, 1990.
- [67] J. Topping, F. D. Giovanni, B. P. Chamberlain, X. Dong, and M. M. Bronstein. Understanding over-squashing and bottlenecks on graphs via curvature. 2021. arXiv:2111.14522 [stat.ML].
- [68] P. van der Hoorn, W. J. Cunningham, G. Lippner, C. Trugenberger, and D. Krioukov. Ollivier-Ricci curvature convergence in random geometric graphs. *Phys. Rev. Research*, 3(1):013211, 2021.
- [69] N. Vishnoi.  $Lx = b$  Laplacian solvers and their algorithmic applications. *Foundations and Trends in Theoretical Computer Science*, 8, 2012.
- [70] U. von Luxburg. A tutorial on spectral clustering. *Statistics and Computing*, 17(4):395–416, 2007.
- [71] U. von Luxburg, A. Radl, and M. Hein. Getting lost in space: Large sample analysis of the commute distance. NIPS’10, page 2622–2630, Red Hook, NY, USA, 2010. Curran Associates Inc.
- [72] U. von Luxburg, A. Radl, and M. Hein. Hitting and commute times in large random neighborhood graphs. *Journal of Machine Learning Research*, 15(52):1751–1798, 2014.
- [73] M. Weber, J. Jost, and E. Saucan. Forman-Ricci flow for change detection in large dynamic data sets. *Axioms*, 5(4):26, 2016.
- [74] M. Weber, J. Stelzer, E. Saucan, A. Naitsat, G. Lohmann, and J. Jost. Curvature-based methods for brain network analysis, 2019. arXiv:1707.00180 [q-bio.NC].
- [75] S. Willerton. Heuristic and computer calculations for the magnitude of metric spaces, 2009. arXiv:0910.5500 [math.MG].
- [76] J. Zhou, Z. Wang, and C. Bu. On the resistance matrix of a graph. *The Electronic Journal of Combinatorics*, 2016.

## Appendix

### A Properties of relative resistance and resistance curvatures

#### A.1 Relative resistance $c_{ij}\omega_{ij}$

We prove the two statements in Property 1:

**Proof of bounds for the relative resistance:** We recall Theorem 2 which says that the relative resistance  $c_{ij}\omega_{ij}$  of a link  $(i, j)$  is equal to the probability that a random spanning tree contains this link. Since  $c_{ij}\omega_{ij}$  is thus a probability, it satisfies  $0 \leq c_{ij}\omega_{ij} \leq 1$ .

We first refine the *lower bound*. By Theorem 1 we know that the effective resistance is a distance and thus that  $\omega_{ij} > 0$  for  $i \neq j$ . We also know that link weights are positive by definition such that we have  $c_{ij}\omega_{ij} > 0$ .

Next, we consider when equality occurs for the *upper bound*. If  $(i, j)$  is a cut link in  $G$ , then any subgraph of  $G$  without  $(i, j)$  is disconnected. Hence, all connected subgraphs (including all spanning trees) of  $G$  must contain  $(i, j)$  and thus  $c_{ij}\omega_{ij} = \Pr[(i, j) \in \mathbf{T}] = 1$ . Hence, if  $(i, j)$  is a cut link then  $c_{ij}\omega_{ij} = 1$ . Conversely, let  $c_{ij}\omega_{ij} = 1$  for some link and assume that it is not a cut link. But then if we consider the *connected* graph  $G' = G \setminus (i, j)$  from which  $(i, j)$  has been removed, we arrive at a contradiction: any spanning tree  $T$  of  $G'$  is also a spanning tree of  $G$  (since  $\mathcal{L}_T \subseteq \mathcal{L}_{G'} \subseteq \mathcal{L}_G$  and  $G'$  is connected) and  $T$  does not contain  $(i, j)$  since it is a subgraph of  $G'$ ; however,  $c_{ij}\omega_{ij} = 1$  implies that  $(i, j)$  is in all spanning trees of  $G$  which contradicts the existence of such a spanning tree  $T$ . Consequently, we know that if  $\omega_{ij}c_{ij} = 1$  then  $(i, j)$  must be a cut link. Together, we have thus shown that  $\omega_{ij}c_{ij} = 1 \Leftrightarrow (i, j)$  is a cut link. This completes the proof.  $\square$

**Proof of Foster's Theorem:** Assume  $G$  is connected. We again use Theorem 2 on the relation between  $c_{ij}\omega_{ij}$  and random spanning trees to rewrite the sum over all relative resistances:

$$\begin{aligned}
\sum_{(i,j) \in \mathcal{L}} c_{ij}\omega_{ij} &= \sum_{(i,j) \in \mathcal{L}} \Pr[(i, j) \in \mathbf{T}] \\
&\stackrel{(a)}{=} \sum_{(i,j) \in \mathcal{L}} \left( \sum_{T \in \mathcal{T}} \Pr[\mathbf{T} = T] \mathbf{1}_{\{(i,j) \in T\}} \right) \\
&= \sum_{T \in \mathcal{T}} \Pr[\mathbf{T} = T] \sum_{(i,j) \in \mathcal{L}} \mathbf{1}_{\{(i,j) \in T\}} \\
&\stackrel{(b)}{=} \sum_{T \in \mathcal{T}} \Pr[\mathbf{T} = T] (n - 1) \\
&= n - 1.
\end{aligned} \tag{13}$$

In step (a) we make the probability expression explicit and in step (b) we use the fact that any spanning tree of a connected graph has  $n - 1$  links, independent of the tree. In brief, this derivation shows that  $\sum_{i \sim j} c_{ij}\omega_{ij}$  equals the average number of links in a spanning tree, which is constant and equal to  $n - 1$ . For a disconnected graph, this result holds for every component independently and as a result we find that the sum over all links in the graph equals  $n - \beta(G)$ ; this completes the proof.  $\square$

Expression (13) can be used for other sums of relative resistances. For instance, since every cycle must at least miss one link in a spanning tree (which is cycle-free) we find that  $\sum_{(i,j) \in \{\text{cycle}\}} \mathbf{1}_{\{(i,j) \in T\}} \leq |\{\text{cycle}\}| - 1$  for any cycle  $\{\text{cycle}\} \subseteq \mathcal{L}$ . Consequently, the sum of relative resistances over a cycle satisfies

$$\sum_{(i,j) \in \{\text{cycle}\}} c_{ij}\omega_{ij} \leq |\{\text{cycle}\}| - 1 \text{ for all cycles.}$$

Similarly, since all spanning trees must have at least one link in a given cut, we find

$$\sum_{(i,j) \in \{\text{cut}\}} c_{ij}\omega_{ij} \geq 1 \text{ for all cuts.} \tag{14}$$

These bounds are an improvement over the straightforward bounds using  $0 < c_{ij}\omega_{ij} \leq 1$ .

## A.2 Node resistance curvature $p$

We prove the two statements in Property 2:

**Proof of  $\sum p_i = \beta$ :** Invoking Foster's Theorem, we can write the sum over all node resistance curvatures as

$$\sum_{i \in \mathcal{N}} p_i = n - \frac{1}{2} \sum_{i \in \mathcal{N}} \sum_{j \sim i} c_{ij}\omega_{ij} = n - \sum_{(i,j) \in \mathcal{L}} c_{ij}\omega_{ij} = \beta,$$

which completes the proof.  $\square$

To prove the node resistance curvature bounds in Property 2, we first show a stronger result:

**Property 4.** *The resistance curvature of a node is bounded by*

$$1 - \frac{d_i}{2} \leq p_i \leq 1 - \frac{\beta(G_i \setminus \{i\})}{2} \text{ for any node } i \in \mathcal{N},$$

where  $G_i \setminus \{i\}$  is the component  $G_i$  with node  $i$  removed. Equality is achieved if and only if all links connected to  $i$  are cut links, in which case both bounds are equal.

**Proof:** The *lower bound* follows immediately from the definition (2) of resistance curvature and the relative resistance bound  $c_{ij}\omega_{ij} \leq 1$  with equality if and only if all incident links are cut links. The *upper bound* follows by summing the relative resistances over cuts: if removing  $i$  disconnects  $G_i$  into  $\beta' := \beta(G_i \setminus \{i\})$  components, this means that the links incident to node  $i$  can be partitioned into  $\beta'$  sets of links  $\{C_k\}_{k=1}^{\beta'}$  which are cuts of  $G_i$ . By the bound (14) for the sum of relative resistances over a cut, we then find

$$p_i = 1 - \frac{1}{2} \sum_{k=1}^{\beta'} \sum_{(i,j) \in C_k} c_{ij}\omega_{ij} \stackrel{(\text{cut bound})}{\leq} 1 - \frac{\beta(G_i \setminus \{i\})}{2}.$$

Next, we consider when equality occurs in the upper bound. First, if all links connected to  $i$  are cut links then we know (a) that their relative resistances are equal to 1 and (b) that  $\beta(G_i \setminus \{i\}) = d_i$  such that  $p_i \leq 1 - d_i/2$ . Since this is equal to the lower bound, we know that equality must hold. To prove *conversely* that equality in the upper bound implies that all links connected to  $i$  are cut links, we will make use of basic facts about spanning trees and cycles in graphs, see for instance [10]. Since the upper bound for  $p_i$  was based on the cut bound (14), we know that if this upper bound holds with equality as  $p_i = 1 - \beta(G_i \setminus \{i\})/2$  then the cut bound (14) must also hold with equality. By equation (13) from which the cut bound follows, this implies that  $\sum_{(i,j) \in C_k} \mathbf{1}\{(i,j) \in T\} = 1$  for all spanning trees  $T$  and all cuts  $C_k$ ; in other words, we find that *every spanning tree has exactly one link in every cut  $C_k$* . If  $n \leq 2$  it then easily follows that the link is a cut link, so assume  $n > 2$ . Let  $T$  be a spanning tree,  $C_k$  a cut and  $\ell = T \cap C_k$  the unique link of  $T$  in the cut  $C_k$ . If we assume that  $|C_k| > 1$  then we may take another link in the cut  $\ell' \in C_k$  and consider the graph  $T + \ell'$ , i.e. the tree with this new link added. This graph will have a unique cycle  $H$  (see [10]) and, since cycles have length at least 3, we can take a link  $\ell'' \in H$  which is different from  $\ell, \ell'$ . But then the graph  $T + \ell' - \ell''$  is again a spanning tree of  $G$  (see [10]) which contains both  $\ell$  and  $\ell'$  i.e. two nodes in the cut  $C_k$ . Since this is in contradiction with every spanning tree having exactly one link in the cut  $C_k$ , we know that  $|C_k| = 1$  which means  $C_k$  is a cut link; this holds for all cuts  $k = 1, \dots, \beta'$ . In other words, if the upper bound holds with equality we know that all links connected to  $i$  are cut links. This completes the proof.  $\square$

**Proof of node resistance curvature bounds:** The upper bound in Property 2 follow as a corollary of Property 4 since  $\beta(G_i \setminus \{i\}) \geq \beta(G_i) = 1$ .  $\square$

Property 4 shows that the resistance curvature is constrained by the combinatorial structure of the graph as neither  $d_i$  nor  $\beta(G_i \setminus \{i\})$  depend on the weights  $c$  in the graph. Furthermore, this gives an example of nodes which have a nonpositive curvature:

**Property 5** (cut nodes). *Cut nodes have nonpositive curvature, with zero curvature if and only if their degree is two.*

**Proof:** If  $i$  is a cut node, then  $\beta(G_i \setminus \{i\}) \geq 2$  and thus by Property 4 it follows that  $p_i \leq 0$ . Next, we consider when zero curvature occurs. Any cut node must have  $d_i > 1$  since otherwise  $i$  is disconnected or a pendant/leaf node and thus not a cut node. If  $i$  is a cut node with  $d_i = 2$ , then the two links incident on  $i$  must be cut links with unit relative resistance and thus  $p_i = 0$ . Conversely, if  $p_i = 0$  for a cut node, then from Property 4 we know that  $\beta(G_i \setminus \{i\}) = 2$  must hold *and* that all links connected to  $i$  must be cut links. This implies that  $d_i = 2$  as required.  $\square$  A related result about cut nodes and the sign of curvature was shown by Fiedler in [24], and follows as a corollary of Property 5:

**Corollary 1.** *If  $G$  has a cut node then either  $G$  is a path graph or  $G$  has a node with negative node resistance curvature.*

**Proof:** Let  $G$  be a graph with cut node  $i$ . Either  $i$  has degree  $d_i > 2$  and thus negative curvature by Property 5, or degree  $d_i = 2$  and zero curvature. If  $d_i = 2$  we furthermore know that the incident links are cut links; hence, if we consider a neighbour of  $i$ , then either (a) this neighbour has degree  $d = 1$ , in which case it is a leaf nodes with  $p = 1/2 > 0$ , or (b) this neighbour has degree  $d = 2$  and both incident links are cut links, such that  $p = 0$  and we may consider its neighbour recursively, or (c) this neighbour has degree  $d > 2$  and either (c1) all incident links are cut links such that  $p = 1 - d/2 < 0$  or (c2) not all incident links are cut links, but then the upper bound in Property 4 is strict and  $p < 0$ . Thus, either we encounter a node with negative curvature or we can recursively consider further neighbours of degree  $d = 2$  until we reach a node of degree  $d = 1$  and stop the process, which would correspond to a path graph. This completes the proof.  $\square$

We mention one additional identity for the node resistance curvature which will be used in the rest of this Appendix: The product of the Laplacian and resistance matrix of a *connected* graph equals

$$Q\Omega = -2I + 2\mathbf{p}\mathbf{u}^T. \quad (15)$$

This identity follows from *Fiedler's identity* [18, 24] and the work of Bapat [6] which relate the Laplacian and resistance matrices of a graph. In particular, we note that this implies that  $\text{diag}(Q\Omega) = 2(\mathbf{p} - \mathbf{u})$ .

### A.3 Link resistance curvature $\kappa$

**Proof of Property 3:** The bounds for the link resistance curvature  $\kappa_{ij}$  in Property 3 follow immediately from the bounds for the node resistance curvature  $p_i$  in Property 2.  $\square$

We can also prove the following stronger result:

**Property 6** (link resistance curvature bounds). *The link resistance curvature is bounded by*

$$\begin{cases} \kappa_{ij} \geq c_{ij}(4 - d_i - d_j) \\ \kappa_{ij} \leq \frac{1}{\omega_{ij}} (6 - 2\beta(G_i \setminus (i, j)) - \beta(G_i \setminus \{i, j\})) \end{cases}$$

*with both bounds achieved (and equal) if and only if all links incident to  $i$  and  $j$  are cut links, and where  $G_i \setminus (i, j)$  is the graph with link  $(i, j)$  removed and  $G_i \setminus \{i, j\}$  the graph with nodes  $i, j$  removed.*

**Proof:** The *lower bound* for the link resistance curvature follows directly from the lower bound  $p_i \geq 1 - d_i/2$  on the node resistance curvature in Property 2 and the bound  $c_{ij}\omega_{ij} \leq 1$  in Property 1, with equality only if all incident links are cut links.

We continue with the *upper bound*. For simplicity, we further assume that  $G = G_i$  is a connected graph – this is without loss of generality since any link will be contained in a unique connected component. We can write the link resistance curvature as

$$\frac{2(p_i + p_j)}{\omega_{ij}} = \frac{1}{\omega_{ij}} \left( 4 - \sum_{l \in \mathcal{L}_{ij}} c_l \omega_l - 2c_{ij}\omega_{ij} \right), \quad (16)$$

where  $\mathcal{L}_{ij} := \{(x, k) \in \mathcal{L} \setminus (i, j) \mid x \in \{i, j\}\}$  are the links incident on  $(i, j)$ . We note that removing nodes  $i$  and  $j$  from  $G$  is equal to removing the links  $\mathcal{L}_{ij}$  from  $G$  and then removing the nodes  $i, j$  from the resulting graph. Hence, every connected component in  $G \setminus \{i, j\}$  is disconnected from

$G$  by some cut  $C_k \subseteq \mathcal{L}_{ij}$ , which gives a partition of  $\mathcal{L}_{ij}$  into cuts. For each cut, we may then invoke the cut bound (14) which yields

$$\sum_{l \in \mathcal{L}_{ij}} c_l \omega_l = \sum_{k=1}^{\beta(G \setminus \{i,j\})} \sum_{l \in C_k} c_l \omega_l \stackrel{(\text{cut bound})}{\geq} \beta(G \setminus \{i,j\}),$$

with equality if and only if all cuts consist of single links (see proof of Property 4) and thus if all links in  $\mathcal{L}_{ij}$  – and thus also  $(i,j)$  – are cut links. Second, we know that the relative resistance satisfies  $c_{ij} \omega_{ij} \geq 0$  and that  $c_{ij} \omega_{ij} = 1$  if and only if  $(i,j)$  is a bridge link. Hence in general we have  $c_{ij} \omega_{ij} \geq [\beta(G \setminus (i,j)) - 1]$  where  $G \setminus (i,j)$  has the link  $(i,j)$  removed; again, equality only holds if this is a cut link. Introducing the bounds for these link terms into (16) yields the proposed upper bound and conditions for equality, and thus completes the proof.  $\square$

## B Resistance curvature and transitivity

Certain graph symmetries have strong implications for the resistance curvatures in a graph. We show this in particular for node and link transitivity<sup>8</sup>.

A permutation  $\pi : \mathcal{N} \rightarrow \mathcal{N}$  of the nodes of a graph is called an *automorphism* if it preserves the graph structure, i.e.  $\pi(i) \sim \pi(j) \Leftrightarrow i \sim j$ . A graph is called *node transitive*<sup>9</sup> if for every two nodes  $i, j$  there exists an automorphism with  $\pi(i) = j$ ; intuitively, this means that all nodes are indistinguishable in the graph since any two nodes may be interchanged without changing the graph structure. Similarly, a graph is called *link transitive* if for every pair of links  $(i,j)$  and  $(x,y)$  there exists an automorphism with  $(\pi(i), \pi(j)) = (x,y)$  (as unordered tuples). See for instance [8] for properties of such graphs. Some common examples of graphs which are node and link transitive are cycle graphs, the complete graph, the hypercube graph and the Platonic graphs (graph skeletons of the Platonic solids); furthermore all *Cayley graphs* are node transitive [8, 29]. For graphs with node and/or link transitivity, we can find the resistance curvature exactly as follows:

**Property 7** (transitivity and curvature). *Let  $G$  be a finite connected graph on  $n$  nodes and  $m$  links and constant link weights  $c$ , then the following hold:*

- *if  $G$  is node transitive, then it has constant resistance curvature equal to  $p = 1/n$ ,*
- *if  $G$  is link transitive with nodes of (possibly equal) degree  $r_1$  and  $r_2$ , then it has constant link resistance curvature equal to  $\kappa = \frac{4cm}{n-1} - c(r_1 + r_2)$ , and*
- *if  $G$  is node and link transitive, then it has constant node and link resistance curvatures equal to  $p = 1/n$  and  $\kappa = 2c\rho$  where  $\rho = m/\binom{n}{2}$  is the link density.*

**Proof: Node transitive** By [8, Proposition 15.2], a permutation  $\pi$  of the nodes of a graph is an automorphism if and only if its corresponding permutation matrix  $P$  leaves the Laplacian matrix invariant, as  $PQP^T = Q$ . Consequently, the structure-preserving row and column permutations of the Laplacian of a node transitive graph will act transitively on the row and column set and we say that the Laplacian is row and column transitive. Since  $G$  is *connected*, the pseudoinverse Laplacian  $Q^\dagger$  is the inverse of the Laplacian in the space  $\text{span}(\mathbf{u})^\perp$  with the permutation-invariant constant vector  $\mathbf{u}$  and we find that  $PQP^T = Q \Rightarrow PQ^\dagger P^T = Q^\dagger$

<sup>8</sup>These are usually called vertex and edge transitivity.

<sup>9</sup>This name refers to the fact that the automorphism group, with automorphisms as group elements and composition ‘ $\circ$ ’ as group operation, acts transitively on the node set.



from:

$$\begin{aligned}
Q^\dagger &= \left( Q + \frac{\mathbf{u}\mathbf{u}^T}{n} \right)^{-1} - \frac{\mathbf{u}\mathbf{u}^T}{n} \quad (\text{see also [27]}) \\
&= \left( PQP^T + \frac{\mathbf{u}\mathbf{u}^T}{n} \right)^{-1} - \frac{\mathbf{u}\mathbf{u}^T}{n} \text{ for all } P \text{ with } PQP^T = Q \\
&= P^T \left[ \left( Q + \frac{\mathbf{u}\mathbf{u}^T}{n} \right)^{-1} - \frac{\mathbf{u}\mathbf{u}^T}{n} \right] P \quad (\text{since } P\mathbf{u} = \mathbf{u} \text{ and } P^{-1} = P^T) \\
&= P^T Q^\dagger P \text{ for all } P \text{ with } PQP^T = Q.
\end{aligned}$$

This also implies that the pseudoinverse Laplacian  $Q^\dagger$  is row and column transitive and consequently that  $Q^\dagger$  has a constant diagonal: for every two nodes  $i, j$  there exists a permutation matrix  $P$  such that  $PQ^\dagger P^T = Q^\dagger$  and  $P\mathbf{e}_i = \mathbf{e}_j$ , and thus

$$(Q^\dagger)_{ii} = \mathbf{e}_i^T Q^\dagger \mathbf{e}_i = \mathbf{e}_i^T PQ^\dagger P^T \mathbf{e}_i = \mathbf{e}_j^T Q^\dagger \mathbf{e}_j = (Q^\dagger)_{jj} \text{ for all } i, j.$$

Thus, the diagonal  $\zeta = \text{diag}(Q^\dagger)$  satisfies  $P\zeta = \zeta$  for any permutation  $P$ . Since we can write the resistance matrix as  $\Omega = \mathbf{u}\zeta^T + \zeta\mathbf{u}^T - 2Q^\dagger$  following definition (1) (see also [18]), this implies that  $PQP^T = Q \Rightarrow P\Omega P^T = \Omega$  and that the resistance matrix is also row and column transitive. From the identity  $Q\Omega = -2I + 2\mathbf{p}\mathbf{u}^T$  in expression (15), we then find that

$$\mathbf{p} = \frac{1}{2} \text{diag}(Q\Omega) + \mathbf{u} = \frac{1}{2} \text{diag}(PQP^T P\Omega P^T) + \mathbf{u} = P\mathbf{p}$$

for all structure-preserving row/column permutations  $P$  of  $Q$ . Since these permutations act transitively on the rows,  $p$  must be constant. By Property 2 we then know that  $\sum_i p_i = np = 1$  and thus that  $p_i = 1/n$  for all nodes.

**Link transitive but not node transitive** If a graph is link transitive and not node transitive, then it must be bipartite on  $\mathcal{V}_1, \mathcal{V}_2$  and the automorphism group acts transitively on these partitions, i.e. the nodes are indistinguishable inside the partitions, see [29, Lemma 3.2.1]. In particular, this implies that all  $(n_1)$  nodes in  $\mathcal{V}_1$  have the same degree  $r_1$  and all  $(n_2)$  nodes in  $\mathcal{V}_2$  have degree  $r_2$ . The number of links is then equal to  $m = n_1 r_1 = n_2 r_2$ . By Foster's theorem and link transitivity – such that  $c_{ij}\omega_{ij}$  must be equal for all links – we find that the effective resistance of every is equal and given by  $\omega = \frac{n-1}{n_1 r_1 c} = \frac{n-1}{n_2 r_2 c}$ . The node curvatures in the two sets then follow as  $p_1 = 1 - \frac{n-1}{2n_1}$  and  $p_2 = 1 - \frac{n-1}{2n_2}$  and the link resistance curvature is then calculated from their sum resulting in the proposed formula for  $\kappa$ .

**Link and node transitive** If the graph is link transitive and node transitive, then  $r_1 = r_2$  in the previous derivation, and from  $c(r_1 + r_2) = 4mc/n$  we then find the proposed link resistance curvature  $2rc/(n-1)$ . An alternative derivation uses the fact that if the graph is node transitive, then  $p_i = 1/n$  as before and that Foster's Theorem together with link transitivity implies that  $\omega = \frac{2(n-1)}{nrc}$  such that  $\kappa = 2rc/(n-1)$  as required. This completes the proof.  $\square$

## C Correspondences between resistance curvature and established discrete curvatures

### C.1 Combinatorial curvature

We show formula (4) which relates the node resistance curvature and combinatorial curvature. Starting from Definition 2 for the resistance curvature and using Theorem 2 for the relation

between relative resistances and spanning trees, we find

$$\begin{aligned}
p_i &= 1 - \frac{1}{2} \sum_{j \sim i} c_{ij} \omega_{ij} \\
&= 1 - \frac{1}{2} \sum_{j \sim i} \sum_{T \in \mathcal{T}} \Pr[\mathbf{T} = T] \mathbf{1}_{\{(i,j) \in T\}} \quad (\text{by Theorem 2}) \\
&= \sum_{T \in \mathcal{T}} \Pr[\mathbf{T} = T] \left( 1 - \frac{1}{2} \sum_{j \sim i} \mathbf{1}_{\{(i,j) \in T\}} \right) \\
&= \sum_{T \in \mathcal{T}} \Pr[\mathbf{T} = T] \left( 1 - \frac{d_i^{(T)}}{2} \right) = \mathbb{E}[p_i^{(co)}(\mathbf{T})],
\end{aligned}$$

where  $d_i^{(T)}$  is the degree of node  $i$  in spanning tree  $T$ . This proves formula (4).

## C.2 Ollivier-Ricci curvature

We prove Proposition 1 which relates the link resistance curvature to Ollivier-Ricci curvature measured with respect to the effective resistance metric and balls  $\mu_{t,i}$  determined by a lazy random walk, i.e. given by the vector  $\mu_{t,i} = (I - Qt)\mathbf{e}_i$ . We will assume  $G$  to be connected, as both  $\kappa$  and  $\kappa^{(OR)}$  are determined in each component independently.

**Proof of Proposition 1:** We start by bounding the Wasserstein distance between the balls  $\mu_{t,i}$  and  $\mu_{t,j}$ :

$$W_1(\mu_{t,i}, \mu_{t,j}) = \min_P \text{tr}(P\Omega) \stackrel{(a)}{\leq} \text{tr}(\mu_{t,i} \mu_{t,j}^T \Omega) \stackrel{(b)}{=} \mu_{t,i}^T \Omega \mu_{t,j}, \quad (17)$$

where for the inequality (a) we have used that  $P = \mu_{t,i} \mu_{t,j}^T$  is a valid matrix for the Wasserstein distance, i.e. with nonnegative entries and the correct marginals, and where equality (b) invokes properties of the trace operator. Introducing the definition of the lazy random walk for  $\mu_{t,i}$  and  $\mu_{t,j}$ , we obtain

$$W_1(\mu_{t,i}, \mu_{t,j}) \leq \mathbf{e}_i^T (I - Qt) \Omega (I - Qt) \mathbf{e}_j \stackrel{(a)}{=} \omega_{ij} - 2t(p_i + p_j) + 2t^2 c_{ij},$$

where in (a) we use the identity  $Q\Omega = -2I + 2\mathbf{p}\mathbf{u}^T$  as in (15). Introduced into the definition of Ollivier-Ricci curvature with  $\omega$  as distance, we then find

$$\kappa_{ij}^{(OR)} = \lim_{t \rightarrow 0^+} \frac{1}{t} \left( 1 - \frac{W_1(\mu_{t,i}, \mu_{t,j})}{\omega_{ij}} \right) \geq \frac{2(p_i + p_j)}{\omega_{ij}}, \quad (18)$$

establishing the bound in Proposition 1.

Next, we show that equality is achieved in the case of cut links. If  $(i, j)$  is a cut link, then  $i$  is a cut node and thus for any two nodes  $x, y$  which are disconnected by removal of  $i$ , we have the triangle equality  $\omega_{xy} = \omega_{xi} + \omega_{iy}$ , see for instance [42]; similarly,  $j$  is a cut node. In particular, the triangle equality will hold for effective resistances between the neighbours of  $i$  and the neighbours of  $j$ , in other words between the supports  $\mathcal{I} := \text{supp}(\mu_{t,i})$  and  $\mathcal{J} := \text{supp}(\mu_{t,j})$  of the balls around  $i$  and  $j$  respectively – where for the lazy random walk we also have  $i \in \mathcal{I}$  and  $j \in \mathcal{J}$ . These effective resistances satisfy  $\omega_{xy} = \omega_{xi} + \omega_{ij} + \omega_{jy}$  for all  $x \in \mathcal{I}, y \in \mathcal{J}$  and consequently, the block matrix  $\Omega_{\mathcal{J}\mathcal{I}}$  has the following low-rank decomposition

$$\Omega_{\mathcal{J}\mathcal{I}} = \omega_j \mathbf{u}^T + \mathbf{u} \omega_i^T + \omega_{ij} \mathbf{u} \mathbf{u}^T$$

where  $\omega_i$  is the  $|\mathcal{I}| \times 1$  vector with effective resistances to the neighbours of  $i$ , as  $(\omega_i)_x = \omega_{ix}$  for  $x \in \mathcal{I}$  and similarly for  $\omega_j$ , and with  $\mathbf{u}$  the all-one vectors of appropriate size. Introducing

this into the expression for the Wasserstein distance, we retrieve

$$\begin{aligned}
W_1(\mu_{t,i}, \mu_{t,j}) &= \min_P \text{tr}(P\Omega) \\
&\stackrel{(a)}{=} \min_P \text{tr}(P_{\mathcal{I}\mathcal{J}}\Omega_{\mathcal{J}\mathcal{I}}) \\
&= \min_P \left( \mathbf{u}^T P_{\mathcal{I}\mathcal{J}} \boldsymbol{\omega}_j + \boldsymbol{\omega}_i^T P_{\mathcal{I}\mathcal{J}} \mathbf{u} + \omega_{ij} \mathbf{u}^T P_{\mathcal{I}\mathcal{J}} \mathbf{u} \right) \\
&\stackrel{(b)}{=} \boldsymbol{\mu}_{t,j}^T \boldsymbol{\omega}_j + \boldsymbol{\omega}_i^T \boldsymbol{\mu}_{t,i} + \omega_{ij} = \boldsymbol{\mu}_{t,i}^T \Omega \boldsymbol{\mu}_{t,j}
\end{aligned}$$

where in step (a) we use that a nonnegative matrix  $P$  with  $\text{supp}(P\mathbf{u}) = \mathcal{I}$  and  $\text{supp}(P^T\mathbf{u}) = \mathcal{J}$  can only have nonzero entries in  $\mathcal{I} \times \mathcal{J}$  and in step (b) we introduce the marginals of  $P$ . This derivation confirms that *equality* is achieved in the Wasserstein inequality (17) and thus also in inequality (18) between the OR curvature and link resistance curvature when  $(i, j)$  is a cut link.  $\square$

### C.3 Forman-Ricci curvature

We show Proposition 2, which relates the link resistance curvature to Forman-Ricci (FR) curvature (6) with a particular choice of weights.

**Proof of Proposition 2:** Starting from the definition of FR curvature (6) with unit weights  $w = 1$ , we find that

$$\kappa_{ij}^{(FR)} = 2 \left( 1 - \frac{1}{2} \sum_{k \sim i} 1 \right) + 2 \left( 1 - \frac{1}{2} \sum_{k \sim j} 1 \right) = 4 - d_i - d_j \stackrel{(a)}{\leq} \frac{\kappa_{ij}}{c_{ij}}$$

where (a) is the lower bound for  $\kappa_{ij}$  in Property 3. This completes the proof.  $\square$

## D Resistance curvature in Euclidean random graphs

We derive formula (8) as an approximation/model of the expected node resistance curvature in Euclidean random graphs. This formula is based on the heuristic (7) for the effective resistance

$$\hat{\omega}_{ij} = \frac{1}{\lambda S(i)} + \frac{1}{\lambda S(j)},$$

where  $S(i)$  is the area of the intersection of the domain  $\mathbb{D}$  and an  $r$ -radius disc around  $i$ . In general, this intersection can take many forms depending on the geometry of the boundary and the location of  $i$  with respect to the boundary, and to overcome this complexity we will make two further assumptions. First, we assume that the curvature of the boundary (as a 1D curve in  $\mathbb{R}^2$ ) is negligible with respect to the curvature of the  $r$ -disc around  $i$ ; if the largest curvature of the boundary is  $1/r_{\mathbb{D}}$  then we assume  $r \ll r_{\mathbb{D}}$ . We remark that in the case of a circular domain of radius  $R$  as in the main text, we have  $r_{\mathbb{D}} = R$  such that the assumption is  $r \ll R$ . With this assumption, we will be able to consider the boundary locally as a straight line (i.e. when considering the neighbourhood around a node). Second, we assume that every point which lies at distance less than  $2r$  from the boundary of  $\mathbb{D}$  has a unique closest point on the boundary. This may be formalized using the concept of *reach* [23, 1] by requiring that the boundary has reach at least  $2r$ . We remark that for a fixed domain  $\mathbb{D}$ , these assumptions will automatically be satisfied if we let  $r$  be small enough.

As Figure 6 illustrates, with these further assumptions  $S(i)$  is determined by the intersection of a disc and a half-plane (due to the straight boundary) and equal to

$$S(i) = \begin{cases} \pi r^2 & \text{if } D_i \geq r \\ A(-D_i) & \text{if } 0 \leq D_i \leq r \end{cases} \quad \text{or, in short } S(i) = A(\max\{-r, -D_i\}) \quad (19)$$

where  $A(t)$  is the area of a circular segment<sup>10</sup> at height  $t$ . In other words, the function  $S$  only depends on the distance from the boundary, and only variations of node position in the direction towards or away from the boundary can change  $S$ ; we may thus further write  $S(D_i)$ . We note that  $A(-r) = \pi r^2$  and  $A(x) + A(-x) = \pi r^2$  for all  $x \in [-r, r]$ .

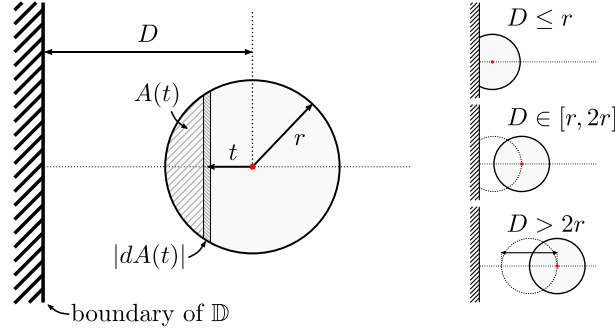


Figure 6: *Illustration of the local neighbourhood around a node in a Euclidean random graph (ERG). By assuming that the boundary curvature is negligible with respect to the curvature of the connection disc around each node as  $r \ll r_{\mathbb{D}}$ , the boundary can be taken as a straight line. **The left figure** shows a node (red point) at distance  $D > r$  from the boundary, the connection disc of radius  $r$  around this node, an example of a circle segment at height  $t$  with area  $A(t)$  and finally  $|dA(t)|$  which is the intersection of points at distance  $D - t$  from the boundary and the connection disc. **The right figure** illustrates the three different node regimes determined by their distance  $D$  to the boundary.*

Now, we fix a distance  $D$  and consider one sample graph  $G$  of the ERG on  $\mathbb{D}$  to which we add a node  $i$  at distance  $D_i = D$  from the boundary. For this node, we can write

$$\begin{aligned}
\hat{p}_i &= 1 - \frac{1}{2} \sum_{j \sim i} \hat{\omega}_{ij} \quad (\text{we consider unweighted ERGs}) \\
&= 1 - \frac{1}{2} \sum_{j \sim i} \left( \frac{1}{\lambda S(D_i)} + \frac{1}{\lambda S(D_j)} \right) \quad (\text{introducing (7) for } \hat{\omega}) \\
&= 1 - \frac{d_i}{2\lambda S(D)} - \frac{1}{2} \sum_{j \sim i} \frac{1}{\lambda S(D_j)} \quad (D_i = D \text{ by construction}) \\
&= 1 - \frac{d_i}{2\lambda S(D)} - \frac{1}{2} \sum_{D'} \frac{\# \text{ neighbours of } i \text{ at distance } D' \text{ from boundary}}{\lambda S(D')},
\end{aligned}$$

where in the last expression  $D'$  sums over  $\{D_j : j \sim i\}$ . As noted,  $S$  only depends on variations in the direction orthogonal to the (straight) boundary. This allows to express the position of the neighbours of  $i$  using the difference  $D - D_j$ , i.e. the distance between  $i$  and  $j$  measured in the direction orthogonal to the boundary. We can write

$$\hat{p}_i = 1 - \frac{d_i}{2\lambda S(D)} - \frac{1}{2} \sum_t \frac{\# \text{ neighbours of } i \text{ at distance } D - t \text{ from the boundary}}{\lambda S(D - t)} \quad (20)$$

where we sum over  $\{t = D - D_j : j \sim i\}$ . We now consider the expectation of  $\hat{p}$  over a random realization of the Euclidean random graph in which node  $i$  is artificially included at the same point in the domain, at distance  $D$  from the boundary. First, the expectation of the degree  $d_i$  is proportional to  $S(D)$  as a property of the Poisson point process, as

$$\mathbb{E}(d_i) = \lambda S(D).$$

<sup>10</sup>This is equal to  $A(t) = r^2 \arccos(t/r) - t\sqrt{r^2 - t^2}$ , and we find  $|dA(t)| = 2\sqrt{r^2 - t^2}$ .

Second, as shown in Figure 6 and as a property of the Poisson process, we find that the expected number of neighbours of node  $i$  at distance  $D - t$  from the boundary is given by  $\lambda|dA(t)|$ . Together, we can write the expectation of (20) as

$$\mathbb{E}(\hat{p}_i) = \frac{1}{2} \left( 1 - \int_{-r}^{\min(r, D)} \frac{|dA(t)|}{S(D-t)} \right), \quad (21)$$

where the range for  $t = D - D_j$  is lower bounded by  $-r$ , which are the neighbours of  $i$  furthest away from the boundary, and upper bounded by  $\min(r, D)$ , which are the neighbours closest to the boundary. Introducing (19) for the function  $S$  retrieves the formula (8) for the expected resistance curvature in Section 4.3. Equation (21) can be integrated numerically for different values of  $D$  as shown in Figure 5.

We can further simplify expression (21) by distinguishing three different cases for  $D$ . Most importantly, this shows that nodes which are sufficiently far away from the boundary will have zero curvature  $\hat{p}_i = 0$  in expectation and thus provides a (heuristic) explanation for the zero resistance curvature tendency in ERGs. The different regimes for  $D$  are as follows:

**Bulk regime** ( $D \geq 2r$ ): In this case we get  $\min(r, D) = r$  and  $S(D-t) = \pi r^2$  for all  $t \in [-r, r]$ , since the neighbours of  $i$  are at least at distance  $r$  from the boundary. From  $\int_{-r}^r |dA(t)| = A(-r)$  we then find that

$$\mathbb{E}(\hat{p}_i) = \frac{1}{2} \left( 1 - \frac{1}{\pi r^2} \int_{-r}^r |dA(t)| \right) = 0 \text{ for } D \geq 2r.$$

**Near-boundary regime** ( $r \leq D \leq 2r$ ): In this case we get  $\min(r, D) = r$  and thus neighbours in the range  $-r \leq t \leq r$  around  $i$ . For these neighbours, we find (a) if  $-r \leq t \leq D - r$  then  $r \leq D - t \leq D + r$  and thus by (19) that  $S(D-t) = \pi r^2$  and (b) if  $D - r \leq t \leq r$  then  $D - r \leq D - t \leq r$  and thus by (19) that  $S(D-t) = A(t-D)$ . Introduced in (21) this yields

$$\begin{aligned} \mathbb{E}(\hat{p}_i) &= \frac{1}{2} \left( 1 - \frac{1}{\pi r^2} \int_{-r}^{D-r} |dA(t)| - \int_{D-r}^r \frac{|dA(t)|}{A(t-D)} \right) \\ &= \frac{1}{2} \left( 1 - \frac{A(-r) - A(D-r)}{\pi r^2} - \int_{D-r}^r \frac{|dA(t)|}{A(t-D)} \right) \\ &= \frac{A(D-r)}{2\pi r^2} - \frac{1}{2} \int_{D-r}^r \frac{|dA(t)|}{A(t-D)} \text{ for } r \leq D \leq 2r. \end{aligned}$$

**Boundary regime** ( $0 \leq D \leq r$ ): In this case we get  $\min(r, D) = D$  and thus neighbours in the range  $-r \leq t \leq D$  around  $i$ . Similar to the near-boundary regime we then find that

$$\begin{aligned} \mathbb{E}(\hat{p}_i) &= \frac{1}{2} \left( 1 - \frac{1}{\pi r^2} \int_{-r}^{D-r} |dA(t)| - \int_{D-r}^D \frac{|dA(t)|}{A(t-D)} \right) \\ &= \frac{A(D-r)}{2\pi r^2} - \frac{1}{2} \int_{D-r}^D \frac{|dA(t)|}{A(t-D)} \text{ for } 0 \leq D \leq r. \end{aligned}$$

To summarize, we find the following piecewise expression

$$\mathbb{E}(\hat{p}(D)) = \begin{cases} \frac{A(D-r)}{2\pi r^2} - \frac{1}{2} \int_{D-r}^D \frac{|dA(t)|}{A(t-D)} & \text{if } D \in [0, r] \\ \frac{A(D-r)}{2\pi r^2} - \frac{1}{2} \int_{D-r}^r \frac{|dA(t)|}{A(t-D)} & \text{if } D \in [r, 2r] \\ 0 & \text{if } D \geq 2r \end{cases}$$

*Remark:* Our analysis of the resistance curvature in ERGs based on  $\mathbb{E}(\hat{p})$  not only explains why we may expect zero resistance curvature in the bulk of ERGs, but it also provides an

explanation for the ‘boundary effect’ in Figures 4 and 5 where we found experimentally that the resistance curvature changes from zero to negative and then positive curvature when nearing the boundary. The analysis above based on  $\hat{\omega}$  shows how this boundary effect originates from the different possible local geometries around a node. This analysis could be relevant in other cases, for instance in [75] where a similar boundary effect was described in the context of the magnitude of graphs (see also [44]), and [11] where the boundary effect was used for boundary detection and related data analysis tasks.

## E Results on the resistance Ricci flow

We first show Proposition 3, which gives a gradient flow expression for the resistance Ricci flow (9). Note that we have assumed  $G$  to be connected such that the resistance matrix  $\Omega$  only contains effective resistances between nodes in the same component.

**Proof of Proposition 3:** We follow the terminology and approach for matrix differentiation used in [57]. For the derivative of some function  $f(\Omega)$  with respect to the resistance matrix  $\Omega$ , one has to account for the specific structure of this matrix. By symmetry and zero diagonal, we have

$$\frac{\partial \Omega}{\partial \omega_{ij}} = (1 - \mathbf{1}_{\{i=j\}})(\mathbf{e}_i \mathbf{e}_j^T + \mathbf{e}_j \mathbf{e}_i^T).$$

The derivative of a function  $f(\Omega)$  with respect to  $\Omega$  is then found from [57]

$$(\nabla_{\Omega} f)_{ij} = \text{tr} \left( \left[ \frac{\partial f}{\partial \Omega} \right]^T \frac{\partial \Omega}{\partial \omega_{ij}} \right),$$

with matrix gradient  $\nabla_{\Omega}$ . As the potential function is a trace with partial derivative  $\partial \text{tr}(\frac{1}{2}\Omega Q \Omega)/\partial \Omega = \frac{1}{2}(Q\Omega + \Omega Q)$ , we find

$$\begin{aligned} (\nabla_{\Omega} \text{tr}(\frac{1}{2}\Omega Q \Omega))_{ij} &= \text{tr} \left( \frac{1}{2}(1 - \mathbf{1}_{\{i=j\}})(Q\Omega + \Omega Q)(\mathbf{e}_i \mathbf{e}_j^T + \mathbf{e}_j \mathbf{e}_i^T) \right) \\ &= (1 - \mathbf{1}_{\{i=j\}}) \left( \mathbf{e}_i^T Q \Omega \mathbf{e}_j + \mathbf{e}_j^T Q \Omega \mathbf{e}_i \right) \\ &= (1 - \mathbf{1}_{\{i=j\}})(2p_i + 2p_j - 4\mathbf{1}_{\{i=j\}}) \quad (\text{by expression (15) for } Q\Omega) \\ &= \begin{cases} 2(p_i + p_j) & \text{if } i \neq j \\ 0 & \text{otherwise} \end{cases} \end{aligned}$$

This confirms that the gradient corresponds to minus the resistance Ricci flow (9), which completes the proof of Proposition 3.  $\square$

*Remark:* with identity (15) for the product  $Q\Omega$ , the potential function can also be written as

$$\text{tr} \left( \frac{1}{2}\Omega Q \Omega \right) = \text{tr} \left( \Omega [\mathbf{p} \mathbf{u}^T - I] \right) = \mathbf{u}^T \Omega \mathbf{p}.$$

As shown in [18] and [19, Appendix I], the node resistance curvature vector  $\mathbf{p}$  satisfies the following equations

$$\begin{cases} \Omega \mathbf{p} = 2\sigma^2 \mathbf{u}, \text{ where} \\ \sigma^2 = \frac{1}{2} \mathbf{p}^T \Omega \mathbf{p} \end{cases} \quad \text{or, equivalently} \quad \begin{cases} \mathbf{p} = \frac{1}{2\sigma^2} \Omega^{-1} \mathbf{u}, \text{ where} \\ \sigma^2 = \frac{1}{2\mathbf{u}^T \Omega^{-1} \mathbf{u}} \end{cases}$$

which allows the potential to be written as  $\text{tr}(\frac{1}{2}\Omega Q \Omega) = 2n\sigma^2$ . The expressions for  $\mathbf{p}$  and  $\sigma^2$  in terms of the inverse resistance matrix are particularly relevant in the context of magnitude [44].

Next, we prove Proposition 4 which gives expression (11) for the resistance Ricci flow in terms

of Laplacian matrices. We again assume  $G$  to be connected for the proof, but the general result follows by combining the Laplacians of each component into a block-diagonal Laplacian matrix. **Proof of Proposition 4:** We will start from expression (11) and show that this flow of Laplacian matrices is equivalent to (9) as a flow of effective resistances. First, for the derivative of the inverse of a matrix we find that  $dA^{-1}/dt = -A^{-1}(dA/dt)A^{-1}$ . Writing the Laplacian pseudoinverse as  $Q^\dagger = (Q + \mathbf{u}\mathbf{u}^T/n)^{-1} - \mathbf{u}\mathbf{u}^T/n$  (see [27]) and considering the flow  $dQ/dt = 2Q \operatorname{diag}(\mathbf{p})Q$ , this yields

$$\begin{aligned} \frac{dQ^\dagger}{dt} &= -Q^\dagger \frac{dQ}{dt} Q^\dagger \\ &= -2Q^\dagger Q \operatorname{diag}(\mathbf{p}) Q Q^\dagger \\ &= -2 \left( I - \frac{\mathbf{u}\mathbf{u}^T}{n} \right) \operatorname{diag}(\mathbf{p}) \left( I - \frac{\mathbf{u}\mathbf{u}^T}{n} \right). \end{aligned}$$

For the change of effective resistances, we then find

$$\frac{d\omega_{ij}}{dt} = (\mathbf{e}_i - \mathbf{e}_j)^T \frac{dQ^\dagger}{dt} (\mathbf{e}_i - \mathbf{e}_j) = -2(p_i + p_j) \text{ for all } i \neq j$$

which confirms that (11) and (9) are equivalent expressions for the resistance Ricci flow.  $\square$